Author(s): ALICE collaboration

Title: Higher harmonic non-linear flow modes of charged hadrons in Pb-Pb collisions at √sNN = 5.02 TeV

Year: 2020

Version: Published version

Please cite the original version:

ALICE collaboration. (2020). Higher harmonic non-linear flow modes of charged hadrons in Pb-Pb collisions at √sNN = 5.02 TeV. Journal of High Energy Physics, 2020(5), Article 85. https://doi.org/10.1007/JHEP05(2020)085

Higher harmonic non-linear flow modes of charged hadrons in Pb-Pb collisions at $\sqrt{s_{\mathrm{NN}}} = 5.02\,\mathrm{TeV}$

The ALICE collaboration

E-mail: ALICE-publications@cern.ch

ABSTRACT: Anisotropic flow coefficients, v_n, non-linear flow mode coefficients, $\chi_{n,mk}$, and correlations among different symmetry planes, $\rho_{n,mk}$ are measured in Pb-Pb collisions at $\sqrt{s_{\mathrm{NN}}} = 5.02\,\mathrm{TeV}$. Results obtained with multi-particle correlations are reported for the transverse momentum interval $0.2 < p_{\mathrm{T}} < 5.0\,\mathrm{GeV}/c$ within the pseudorapidity interval $0.4 < |\eta| < 0.8$ as a function of collision centrality. The v_n coefficients and $\chi_{n,mk}$ and $\rho_{n,mk}$ are presented up to the ninth and seventh harmonic order, respectively. Calculations suggest that the correlations measured in different symmetry planes and the non-linear flow mode coefficients are dependent on the shear and bulk viscosity to entropy ratios of the medium created in heavy-ion collisions. The comparison between these measurements and those at lower energies and calculations from hydrodynamic models places strong constraints on the initial conditions and transport properties of the system.

KEYWORDS: Heavy Ion Experiments

Contents

1 Introduction

One of the primary goals in the ultra-relativistic heavy-ion collision programs at the Relativistic Heavy Ion Collider (RHIC) and the Large Hadron Collider (LHC) is to study the nuclear matter at extreme conditions. The pressure gradients in the strongly interacting matter, known as the Quark-Gluon Plasma (QGP), are believed to drive the hydrodynamic expansion observed through anisotropy in multi-particle correlations in high energy collisions at RHIC and the LHC [1, 2]. The anisotropic expansion of the medium, commonly referred to as anisotropic flow [1], can be characterized by a Fourier decomposition of the azimuthal particle distribution with respect to the reaction plane [3, 4]

$$\frac{\mathrm{d}N}{\mathrm{d}\varphi} \propto 1 + 2\sum_{n=1}^{\infty} v_n \cos(n(\varphi - \psi_{\mathrm{RP}})), \tag{1.1}$$

where the flow coefficient v_n is the magnitude of the n-th order flow, and the reaction plane ψ_{RP} defined by the beam direction and impact parameter which is defined as the distance between the centers of two colliding nuclei. Due to fluctuations in the initial state energy density profile, it is useful to define symmetry planes of different orders, where the n-th order plane ψ_n defines the orientation of the n-th order complex flow vector $V_n \equiv v_n \mathrm{e}^{in\psi_n}$. The expansion of the azimuthal distribution about ψ_n also yields finite values of odd coefficients [5, 6]. Anisotropic flow measurements through two- and multi-particle azimuthal correlations [6–13] have provided important information on the medium response and in particular its transport coefficients such as the shear viscosity to entropy density ratio (η/s), bulk viscosity to entropy density ratio (ζ/s) and the equation of state [14]. Studies have shown the relativistic hydrodynamic nature of the medium [1, 2, 15–22], with η/s close to the AdS/CFT minimum $1/(4\pi)$ [23].

The initial state eccentricity, determined from the energy density profile, is obtained from the definition [5]

$$\varepsilon_n e^{in\Phi_n} = -\{r^n e^{in\varphi}\}/\{r^n\}, \, n \geq 2, \tag{1.2}$$

where the curly brackets denote the average over the transverse plane, i.e. $\{\cdots\} = \int \mathrm{d}x \mathrm{d}y \, e(x, y, \tau_0)(\cdots)$, r is the distance to the system's center of mass, φ is the azimuthal angle, $e(x, y, \tau_0)$ is the energy density at the initial time τ_0, and Φ_n is the participant plane angle, defining the spatial symmetry of the nuclear constituents in the participant region (see refs. [24, 25]). Hydrodynamic models demonstrate that the second and the third harmonic flow coefficients exhibit an almost linear dependence on the initial eccentricity coefficients ε_n [26]. Considering that the anisotropic expansion is a result of a hydrodynamic evolution governed by η/s, a measurement of the second and third harmonics combined with hydrodynamic calculations can constrain the properties of the medium. Several estimates for the limits of η/s were determined through measurements of elliptic flow coefficient v_2 [27–32] and their comparison with hydrodynamic calculations. Consequently, the early constraints placed the value of η/s between 0.08 to 0.16 [33–35]. However, the limited sensitivity of the elliptic flow to η/s and the large uncertainty in the initial state anisotropy inhibit a precise determination of the value of η/s [34, 36–38], and its temperature dependence, which was recently shown to be explorable during the second run of LHC [39, 40]. In addition, part of the anisotropic flow can also originate from the hadronic phase [41–43]. It has been shown in [43, 44] that the inclusion of the temperature dependent bulk viscosity $\zeta/s(\mathrm{T})$ in hydrodynamic simulation lead to a better description of the average transverse momentum of charged hadrons and on the elliptic flow coefficient. The effects of bulk viscosity should be considered when extracting any transport coefficient from the data [45–47].

Flow harmonics of order $n \geq 3$ reveal finer details of initial conditions [6, 8, 10, 11, 13], enabling to constrain η/s better [39, 40, 48, 49]. Higher flow harmonics $n > 3$ do not exhibit a linear response to the initial anisotropy [26] as a finite contribution is induced by the initial state anisotropy of the lower orders [50, 51]. For example, the fourth order flow vector V_4 gains contributions not only from the fourth order flow (linear flow mode), but also from the second order flow (non-linear flow mode). Starting from the V_n estimators studied in [50], the flow can be expressed as a vector sum of the linear and non-linear modes

$$
\begin{aligned}
V_4 &= V_{4\mathrm{L}} + \chi_{4,22} V_2^2, \\
V_5 &= V_{5\mathrm{L}} + \chi_{5,23} V_2 V_3, \\
V_6 &= V_{6\mathrm{L}} + \chi_{6,222} V_2^3 + \chi_{6,33} V_3^2 + \chi_{6,24} V_2 V_{4L}, \\
V_7 &= V_{7\mathrm{L}} + \chi_{7,223} V_2^2 V_3 + \chi_{7,34} V_3 V_{4L} + \chi_{7,25} V_2 V_{5L}, \\
V_8 &= V_{8\mathrm{L}} + \chi_{8,2222} V_2^4 + \chi_{8,233} V_2 V_3^2 + \mathcal{E}(V_{4L}, V_{5L}, V_{6L}),
\end{aligned}
\tag{1.3}
$$

where $\chi_{n,mk}$ is called non-linear flow mode coefficient, characterizing the non-linear flow mode induced by the lower order harmonics. The high order linear component is denoted by $V_{n\mathrm{L}}$, while the many higher order linear couplings are depicted by $\mathcal{E}(\dots)$ for V_8. The

$V_{n\mathrm{L}}$ is linearly related to a cumulant-defined anisotropy [52]

$$\varepsilon'_4 \mathrm{e}^{i4\Phi'_4} = \varepsilon_4 \mathrm{e}^{i4\Phi_4} + \frac{3\langle r^2 \rangle^2}{\langle r^4 \rangle} \varepsilon_2 \mathrm{e}^{i4\Phi_2} \tag{1.4}$$

as opposed to the relation $v_n \propto \varepsilon_n$, where v_n is the magnitude of the total contribution and ε_n is given by eq. (1.2).

In earlier measurements performed by ALICE [53], the non-linear flow mode coefficients were measured up to the sixth harmonic order in Pb-Pb collisions at $\sqrt{s_{\mathrm{NN}}} = 2.76\,\mathrm{TeV}$. It was indicated that the coefficients $\chi_{5,23}$ and $\chi_{6,33}$ are sensitive not only to η/s, but also to the distinctive energy density profiles generated by different initial conditions. It was observed that the hydrodynamic models with their respective initial conditions Monte-Carlo (MC)-Glauber [54, 55], MC-KLN [33, 56], and IP-Glasma [57]), are unable to reproduce these measurements, which indicates that the model tuning and η/s parameterization require further work.

In this paper, measurements of high order flow coefficients in Pb-Pb collisions at $\sqrt{s_{\mathrm{NN}}} = 5.02\,\mathrm{TeV}$ are presented. The flow coefficients v_n are measured up to the ninth harmonic, v_9, extending the previous measurements of v_2–v_6 [58]. The data recorded during the 2015 heavy-ion run of the LHC allow the measurements of non-linear flow mode and correlations between symmetry planes to be extended. A total of six non-linear flow mode coefficients are measured, including the non-linear flow mode coefficient $\chi_{7,223}$, for which the sensitivity to η/s is expected to be significantly stronger than for the lower odd-harmonic coefficient $\chi_{5,23}$ [37, 59]. The results are compared with those in Pb-Pb collisions at $\sqrt{s_{\mathrm{NN}}} = 2.76\,\mathrm{TeV}$ [53] and various state of the art hydrodynamical calculations.

2 Formalism and observables

In order to separate the linear and non-linear contributions from eq. (1.3), one assumes the respective contributions to be uncorrelated [60]. For example for the fourth order V_4, by mean-squaring the equations in eq. (1.3) and setting $\langle (V_2^*)^2 V_{4L} \rangle \simeq \langle V_2^2 V_{4L}^* \rangle \simeq 0$, the linear part can be derived

$$\underbrace{\langle |V_{4L}|^2 \rangle^{\frac{1}{2}}}_{v_{4\mathrm{L}}} = (\underbrace{\langle |V_4|^2 \rangle}_{v_4^2} - \underbrace{\chi_{4,22}^2 \langle |V_2|^4 \rangle}_{v_{4,\mathrm{NL}}^2})^{\frac{1}{2}}. \tag{2.1}$$

Here $\langle \rangle$ denotes an average over all events and * the complex conjugate. The magnitudes of the linear and non-linear flow coefficients are denoted with $v_{4\mathrm{L}}$ and $v_{4,\mathrm{NL}}$, respectively.

The observables of the non-linear response mode are constructed from the projections of flow vectors on to the symmetry planes of lower harmonics [61, 62]. For $n = 4$, the magnitude of the non-linear response mode is given by

$$v_{4,22} = \frac{\Re \langle V_4 (V_2^*)^2 \rangle}{\sqrt{\langle |V_2|^4 \rangle}} \approx \langle v_4 \cos(4\psi_4 - 4\psi_2) \rangle, \tag{2.2}$$

where $v_{4,22}^2 \equiv v_{4,\mathrm{NL}}^2 \equiv \chi_{4,22}^2 \langle |V_2|^4 \rangle$. The right-hand side approximation holds if the low $(n = 2, 3)$ and high order flow is weakly correlated. Only the fourth harmonic is shown here and the complete list of other harmonics are provided in appendix A.

The contributions from short-range correlations unrelated to the common symmetry plane, commonly referred to as "non-flow", are suppressed by using the subevent method where the event is divided into two subevents separated by a pseudorapidity gap [4]. The underlying multi-particle correlation coefficient for subevent A is $v_{4,22}^{A} = \langle\langle\cos(4\varphi_1^{A} - 2\varphi_2^{B} - 2\varphi_3^{B})\rangle\rangle / \langle\langle\cos(2\varphi_1^{A} + 2\varphi_2^{A} - 2\varphi_3^{B} - 2\varphi_4^{B})\rangle\rangle^{1/2}$ as determined using eq. (2.2),[1] and a similar treatment is applied for the subevent B, for which $v_{4,22}^{B}$ is obtained by swapping B for A in the aforegiven expression. The final result is then the average of the results from subevents A and B.

The symmetry-plane correlations are defined as the ratio between the magnitude of the non-linear flow modes and flow coefficients [63]. For $n = 4$, one obtains

$$\rho_{4,22} = \frac{v_{4,22}}{v_4} \approx \langle\cos(4\psi_4 - 4\psi_2)\rangle. \tag{2.3}$$

A value close to zero indicates weakly correlated symmetry planes, while a value reaching one implies a strong correlation. The correlations between symmetry planes reflect those of the corresponding initial state participant planes [53, 64], therefore providing valuable information on the evolution of the QGP. Correlations between symmetry planes have been previously studied using the event-plane method [64, 65], *event plane* describing an experimentally approximated symmetry plane. However, these results depend on the event-plane resolution [66], which complicates the comparison between data and theoretical calculations. Recently, the ALICE Collaboration has measured symmetry-plane correlations [53]. It was found that the correlations of symmetry planes of higher harmonics with second and third order symmetry planes increased for less central collisions. Furthermore, the comparison with hydrodynamic calculations revealed the importance of final-state collective dynamics in addition to the initial-state density fluctuations [33] as it is known that the observation of correlated final state symmetry planes implies the existence of fluctuations in the initial state eccentricity vectors.

The fourth non-linear flow mode coefficient, with the aforementioned assumptions, is given by [59]

$$\chi_{4,22} = \frac{v_{4,22}}{\sqrt{\langle v_2^4 \rangle}}. \tag{2.4}$$

3 Experimental setup and data analysis

The data sample consists of about 42 million minimum bias Pb-Pb collisions at $\sqrt{s_{NN}} = 5.02\,\text{TeV}$, recorded by ALICE [67, 68] during the 2015 heavy-ion run at the LHC. Detailed descriptions of the detector can be found in [67, 69, 70]. The trigger plus crossing of beam is provided by signals from the two scintillator arrays, V0A and V0C [67, 71], covering the pseudorapidity intervals $2.8 < \eta < 5.1$ and $-3.7 < \eta < -1.7$, respectively. A primary vertex position less than 10 cm in beam direction from the nominal interaction point is required. Pile-up events are removed by correlating the V0 multiplicity with the multiplicity from the first Silicon Pixel Detector (SPD) [67, 72] layer. To further remove pile-up events,

---

[1]For practical usage, the self-correlation is recursively removed from three- and four-particle correlations, resulting in modified equations.

information from the Time-of-Flight (TOF) [73] detector is used: the multiplicity estimates from the SPD are correlated with those imposed with a TOF readout requirement. The centrality of the collision is determined using information from the V0 arrays. Further details on the centrality determination in ALICE are given in [74]. Only events in the centrality range 0% to 60% are used in the analysis.

The track reconstruction is based on combined information from the Time Projection Chamber (TPC) [67, 75] and the Inner Tracking System (ITS) [67, 72]. To avoid contributions from secondary particles, the tracks are required to have a distance of closest approach to the primary vertex of less than 3.2 cm and 2.4 cm in the longitudinal and transverse directions, respectively. Such a loose Distance of Closest Approach (DCA) track cut is chosen to improve the uniformity of the φ-distribution for the Q_n-vector calculation. Furthermore, each track is required to have at least 70 TPC space points out of the maximum 159, and the average χ^2 per degree of freedom of the track fit to the TPC space points to be less than 2. Minimum 2 hits are required in the ITS. In order to counteract the effects of track reconstruction efficiency and contamination from secondary particles [76], a HIJING simulation [77, 78] with GEANT3 [79] detector model is employed to construct a p_T-dependent track weighting correction. The track reconstruction efficiency is approximately 65% at $p_T = 0.2 \, \text{GeV}/c$ and 80% at $p_T > 1.0 \, \text{GeV}/c$, while the contamination from secondaries is less than 10% and 5%, respectively. Only particle tracks within the transverse momentum interval $0.2 < p_T < 5.0 \, \text{GeV}/c$ and pseudorapidity range $0.4 < |\eta| < 0.8$ are considered. A pseudorapidity gap $|\Delta \eta| > 0.8$ is used to suppress the non-flow. The observables in this analysis are measured with multi-particle correlations obtained using the generic framework for anisotropic flow analysis [80].

4 Systematic uncertainties

The systematic uncertainties are estimated by varying criteria for selecting the events and tracks. The systematic evaluation is done by independently varying the selection criteria, and the results given by this variation are then compared to the default criteria given in section 3. The total uncertainty is obtained by assuming that the individual sources are uncorrelated, which are then quadratically summed.

Summaries of the relative systematic uncertainties are given in tables 1–4. Uncertainties stemming from the event selection criteria are estimated by changing the rejection based on the vertex position from 10 cm to 8 cm and by adjusting the pile-up rejection criteria. It is found that the contribution to the uncertainty is generally negligible, below 1%. An alternative centrality determination is employed using the event multiplicity estimates from the SPD layers. The uncertainty related to the centrality determination is less than 2% for all observables, except for v_7 to v_9 for which the uncertainty increases to 10%.

The ALICE detector can be operated with either positive or negative solenoid magnetic field polarity. The polarity of the field affects the direction of the charged particle curvature, while also subjecting the structural materials of the detector itself to either a positive or negative magnetic field. The default data set is composed of events recorded with both polarities. The results produced with exclusively either negative or positive magnetic field configurations deviate from the default by up to 15% in case of flow coefficients, and 28% for

Type	v_2	v_3	v_4	v_5	v_6	v_7	v_8	v_9
Event Selection								
z-vertex cut	< 0.1	< 0.1	< 0.1	0.5	1.2	1.6	1.8	1.7
Pile-up rejection	< 0.1	< 0.1	< 0.1	0.2	0.8	1.3	1.7	2.0
Centrality Determination								
SPD	0.6	0.3	0.3	1.1	3.9	6.6	9.1	11.5
Tracking								
Magnetic field polarity	0.1	0.1	1.7	2.4	4.1	6.8	10.5	15.2
Tracking mode	0.1	0.2	< 0.1	2.4	5.4	7.2	7.6	6.8
Number of TPC space points	0.7	1.2	1.4	1.5	1.6	1.7	1.7	1.8
Space charge distortion	< 0.1	< 0.1	< 0.1	0.2	0.7	1.2	1.7	2.3
Non-flow								
Charge combinations ($--/++$)	1.1	0.7	0.8	2.9	6.2	9.3	12.3	15.2
Overall	1.5	1.4	2.4	4.9	10.3	15.4	20.4	25.6

Table 1. Relative systematic uncertainties of the flow coefficients. The uncertainties are given in percents and are categorized into four groups: event selection, centrality determination, tracking and non-flow. The overall systematic uncertainty is obtained by summing in quadrature the uncertainties from each source.

Type	$v_{4,22}$	$v_{5,23}$	$v_{6,222}$	$v_{6,33}$	$v_{6,24}$	$v_{7,223}$
Event Selection						
z-vertex cut	0.1	0.1	0.2	0.3	0.2	0.1
Pile-up rejection	< 0.1	0.1	0.4	0.5	0.4	< 0.1
Centrality Determination						
SPD	1.5	0.7	0.3	0.3	0.7	1.4
Tracking						
Magnetic field polarity	0.5	0.5	1.9	3.2	4.4	5.5
Tracking mode	0.1	0.4	1.4	1.7	1.1	< 0.1
Number of TPC space points	3.8	2.3	1.5	1.4	2.1	3.5
Space charge distortion	0.2	0.1	1.8	4.0	6.7	9.9
Non-flow						
Charge combinations ($--/++$)	4.2	4.7	5.8	7.4	9.6	14.3
Overall	5.9	5.3	6.7	9.3	12.7	18.6

Table 2. Relative systematic uncertainties of the harmonic projections $v_{n,mk}$.

$\rho_{7,223}$. In order to estimate the non-flow contributions from resonance decays, the like-sign technique [2] which correlates exclusively either positively or negatively charged particles, is employed. The difference with respect to the results obtained by selecting all charged particles is assigned as a systematic uncertainty. In general, this uncertainty ranges from 2% to 15%. The effect from the space charge distortions in the TPC drift volume because

Type	$\rho_{4,22}$	$\rho_{5,23}$	$\rho_{6,222}$	$\rho_{6,33}$	$\rho_{6,24}$	$\rho_{7,223}$
Event Selection						
z-vertex cut	0.1	0.3	0.1	0.2	0.8	2.5
Pile-up rejection	0.1	0.3	0.1	0.3	1.0	2.2
Centrality Determination						
SPD	0.9	0.3	0.7	0.9	1.2	1.5
Tracking						
Magnetic field polarity	< 0.1	1.8	6.8	10.1	13.8	18.0
Tracking mode	0.1	0.3	0.8	2.6	6.1	11.2
Number of TPC space points	< 0.1	0.7	0.1	< 0.1	1.0	2.8
Space charge distortion	0.2	0.2	1.5	3.5	6.7	11.1
Non-flow						
Charge combinations $(--/++)$	3.1	3.6	3.6	5.6	8.7	12.9
Overall	3.3	4.2	7.9	12.4	18.8	27.5

Table 3. Relative systematic uncertainties of the symmetry-plane correlations $\rho_{n,mk}$.

Type	$\chi_{4,22}$	$\chi_{5,23}$	$\chi_{6,222}$	$\chi_{6,33}$	$\chi_{6,224}$	$\chi_{7,223}$
Event Selection						
z-vertex cut	< 0.1	0.1	0.3	0.3	0.3	0.1
Pile-up rejection	< 0.1	0.1	0.5	0.6	0.5	0.1
Centrality Determination						
SPD	0.2	0.6	1.0	1.0	0.7	0.1
Tracking						
Magnetic field polarity	0.6	0.2	2.5	4.1	5.1	5.5
Tracking mode	< 0.1	0.2	1.4	1.7	1.2	0.2
Number of TPC space points	< 0.1	0.2	0.5	0.7	0.9	1.1
Space charge distortion	0.2	0.1	1.9	4.4	7.1	10.1
Non-flow						
Charge combinations $(--/++)$	0.2	1.5	7.7	12.0	14.4	15.0
Overall	0.7	1.7	8.5	13.6	17.0	19.0

Table 4. Relative systematic uncertainties of the non-linear flow mode coefficients $\chi_{n,mk}$.

of the higher interaction rates is estimated by comparing results from different regions of the TPC, one for $\eta > 0$ and the other $\eta < 0$. The maximum uncertainty is evaluated less than 15%. The track reconstruction related uncertainty, referred to as tracking mode, is evaluated by comparing the results obtained with tracks for which the requirement for the number of hits in the ITS layers is changed. In this case, the uncertainty is generally less than 15%, and a maximum 20% is evaluated for $\rho_{7,223}$. Furthermore, the track selection criteria is tightened by increasing the minimum number of the TPC space points from 70 to 90, resulting in uncertainties around 1% to 3%.

5 Results

In this section, the measurements of the flow coefficients, the non-linear modes, symmetry-plane corre-lations and the non-linear flow mode coefficients are presented. They are compared with hydrodynamic calculations with various settings [25, 57, 81, 82]. The first calculation is based on an event-by-event viscous hydrodynamic model with EKRT initial conditions [25, 81] using a value of $\eta/s = 0.20$ (param0) and a temperature dependent $\eta/s(T)$ (param1). For both configurations, ζ/s is set to zero. The visualization of the model parameters can be found in figure 1. The second calculation employs the iEBE-VISHNU hybrid model [83] with AMPT [84–86] and TRENTo [87] initial conditions. The $\eta/s = 0.08$ and $\zeta/s = 0$ are taken for param2, while the $\eta/s(T)$ and $\zeta/s(T)$ (param3), extracted using Bayesian analysis [45] (except for the normalization factors) from a fit to the final multiplicities of the charged hadron spectra in Pb-Pb collisions at $\sqrt{s_{NN}} = 5.02$, are used for the TRENTo initial conditions. The third calculation uses the MUSIC model [88] with IP-Glasma [89] initial conditions with a value of $\eta/s = 0.095$ and $\zeta/s(T)$ (param4). Each of the $\eta/s(T)$ parameterizations is adjusted to reproduce the measured charged hadron multiplicity, the low-p_T region of the charged-hadron spectra, and v_n from central to mid-peripheral collisions up to the fourth harmonic at RHIC and the LHC [25, 44, 57, 84, 90–92]. The model configurations are summarized in table 5.

In figure 2, the measurements of the flow coefficients from v_2 to v_9 are presented. The first two coefficients up to v_6 have been extensively measured at RHIC and LHC [6–13], and more recently also v_7 [49]. The present analysis reports the first results on higher harmonic coefficients from v_7 to v_9 in ALICE, where v_8 and v_9 are measured for the first time at the LHC energies. The coefficients exhibit a modest centrality dependence, and their magnitude is similar to that of v_7 within statistical and systematic uncertainties. The measurements up to v_6 are compatible with those published previously [58].

Figure 2 also shows the comparison between the measured v_n and model calculations. The hydrodynamic calculations qualitatively reproduce the v_n measurements, and the overall model depiction is very good for v_2 and v_3. For $n \geq 4$ however, the calculations show noticeable overestimations, especially in mid-peripheral collisions. For v_5 and v_6, the data are well described by EKRT+param0, showing a better agreement than the temperature dependent EKRT+param1. The data are also described by AMPT+param2, for which the agreement for v_5 and v_6 is good in mid-central and mid-peripheral collisions. IP-Glasma+ param4 and TRENTo+param3 overestimate the measurements by a factor of 1.5∼2. Values of v_7 are well estimated by AMPT+param2, and v_8 by both AMPT+param2 and TRENTo+param3 within uncertainties. In other cases, the data are overestimated by the other models.

To study the dependence on the harmonic order of the anisotropy coefficients [97], figure 3 shows values of different coefficients as a function of n for all centralities. This presentation is particularly well suited in visualizing the harmonic dependence, and the acoustic scaling [97] observed across the harmonic orders. The decrease in v_n with increasing harmonic order up to $n = 7$ indicates viscous damping [97]. This means that the higher frequency waveform propagating through the medium should get more damped
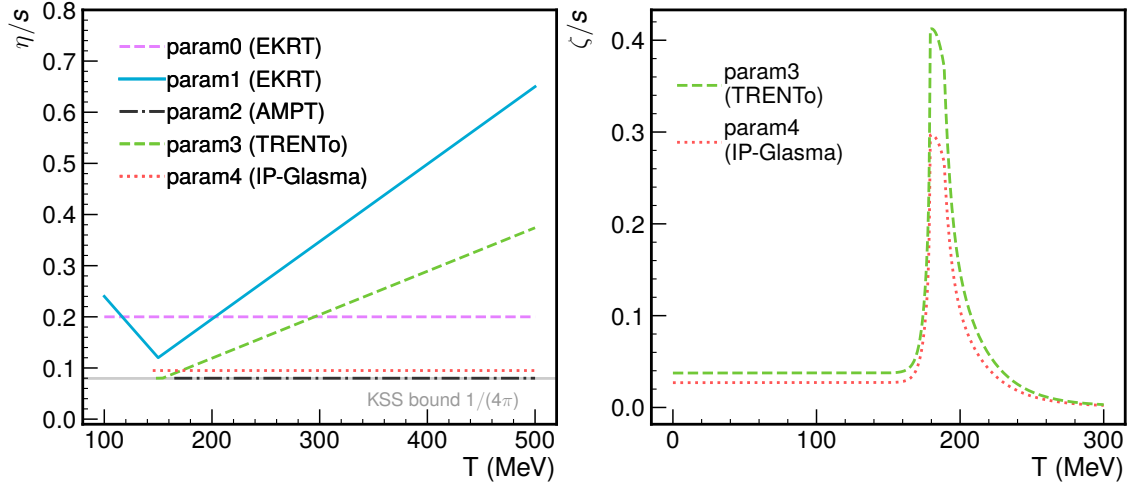
Figure 1. The five different parameterizations of η/s and ζ/s used for the different hydrodynamic model calculations are shown in the left and right panel. Note that the functional form of $\zeta/s(T)$ is the same for param3 and param4 and taken from eq. 5 in [45] motivated by refs. [43, 93–95]. For the parameters with TRENTo initial condition, the ones based on identified yields are taken from table 4 in [45]. The ζ/s normalization factor used with IP-Glasma (TRENTo) initial conditions is 0.9 (1.25). The models with $\zeta/s = 0$ are not shown on the right.

Model	Hydrodynamic code	Initial conditions	η/s	ζ/s
EKRT+param0 [25, 81]	EbyE [25, 96]	EKRT [25, 81]	0.20	0
EKRT+param1 [25, 81]	EbyE [25, 96]	EKRT [25, 81]	$\eta/s(T)$ [25]	0
AMPT+param2 [82]	iEBE-VISHNU [83]	AMPT [84–86]	0.08	0
TRENTo+param3 [82]	iEBE-VISHNU [83]	TRENTo$(p=0)$ [87]	$\eta/s(T)$ [45, 82]	$\zeta/s(T)$ [45, 82]
IP-Glasma+param4 [57]	MUSIC [88]	IP-Glasma [89]	0.095	$\zeta/s(T)$ [57]

Table 5. Hydrodynamic model configurations. Shown are the key components such as initial condition models, and η/s and ζ/s parameterizations. With TRENTo initial conditions, an entropy deposition parameter $p = 0$ [82] is used for all calculations.

until freeze-out takes place. In [98, 99] the viscosity effect is explained as the main contributor to the observed damping. It is speculated, that another driving factor is the phase of the oscillation itself, which also contributes to the magnitude at the time of freeze-out. The measurements show that there is a hint of $v_9 > v_8$, as also predicted in the acoustic model [97].

Figure 4 presents the higher order flow coefficients as well as their linear and non-linear flow modes up to the seventh order as a function of centrality. For the flow harmonics v_4 and v_5, presented in panels (a) and (b), respectively, the non-linear contributions are small in central collisions, where the linear contribution is dominant. A weak centrality dependence is observed for the linear component. In case of v_4, significant contributions from the second order arise in less central collisions. The v_5 coefficient, on the other hand, is largely induced by the low order v_2 and v_3, indicated by the large $v_{5,23}$.
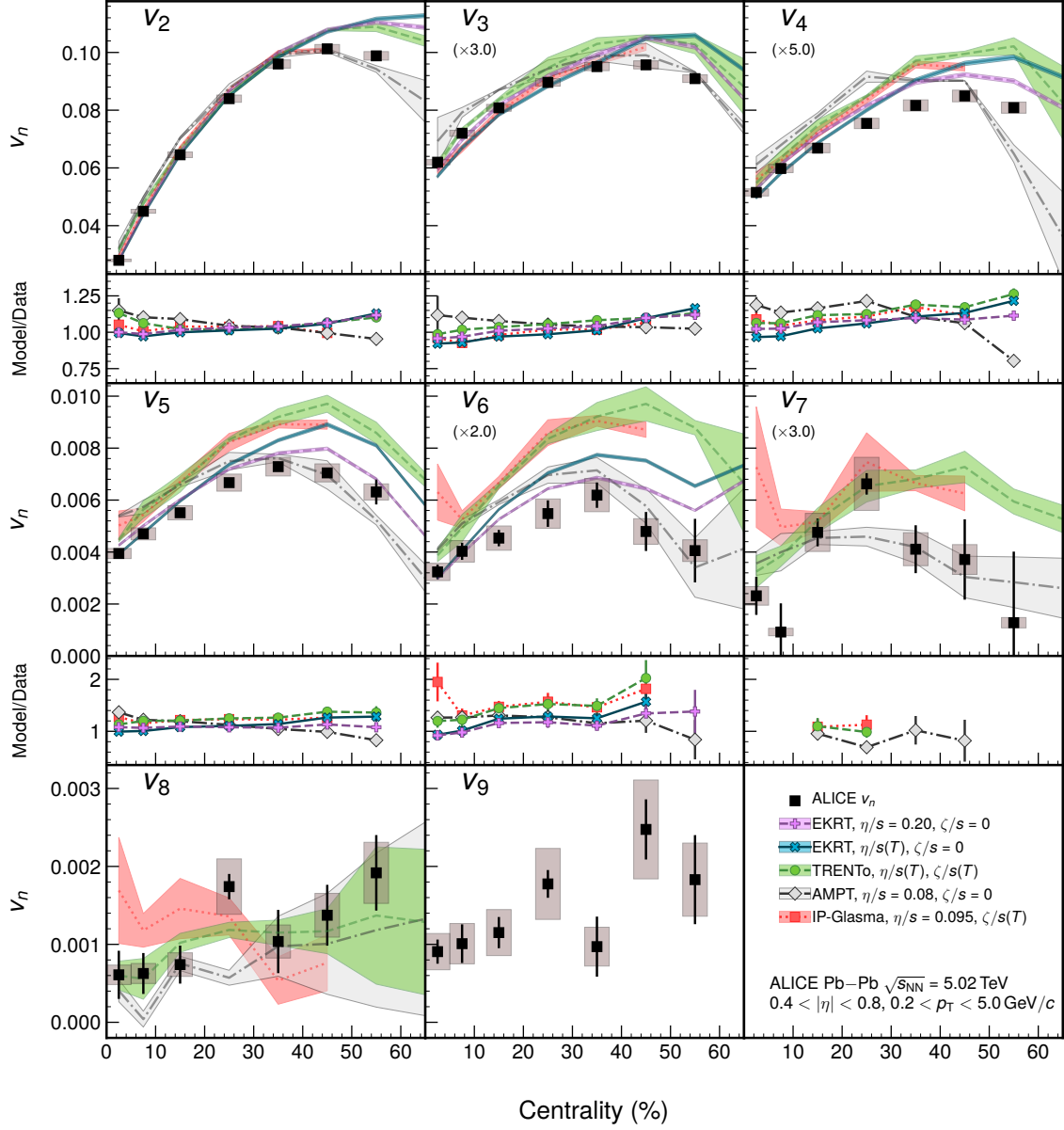
Figure 2. Flow harmonics up to the ninth order as a function of centrality, along with five different hydrodynamic calculations shown as color bands, each representing different configurations. For the black markers representing the measured data points, the sytematic uncertainty is indicated by the gray patches around the markers. The bands indicate the extent of the uncertainty of the corresponding calculation. On the bottom part of each panel, the ratios between model calculations and the data are shown with symbols. Ratios with uncertainties larger than 1 are not shown in the ratio panel. For some panels, the points are scaled by an indicated factor for better visibility across the panels.
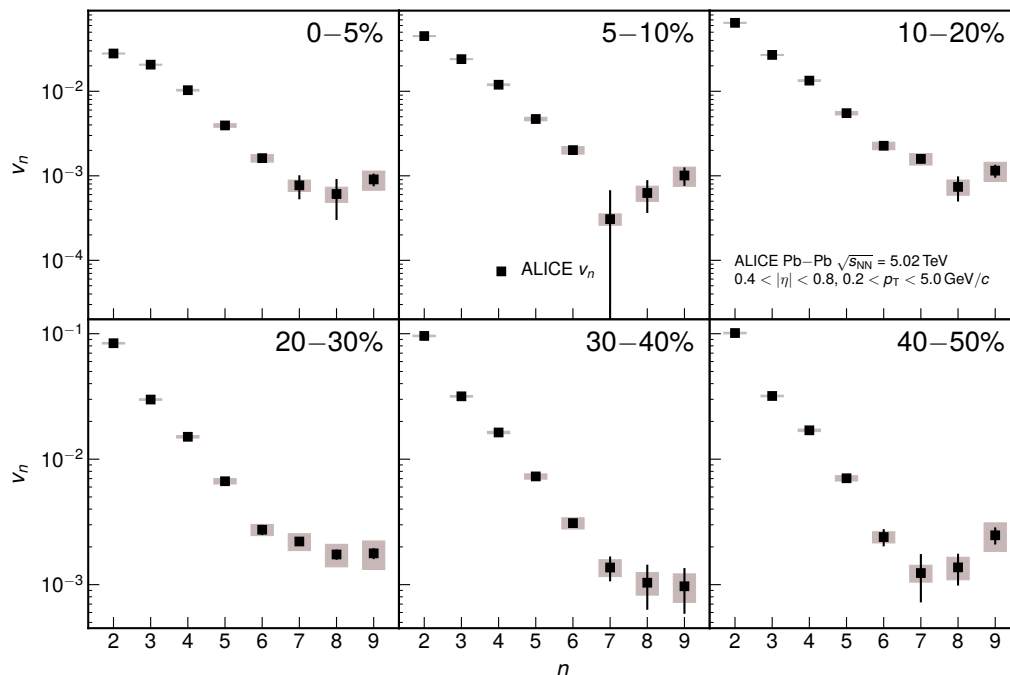
Figure 3. v_n as a function of the harmonic order n for various centrality intervals.

Panels (c) and (d) of figure 4 show the flow modes of v_6 and v_7. Only the non-linear flow modes of v_6 and v_7 are presented. The $v_{6,222}$ increases from zero to approximately half of the total v_6 in mid-central collisions, while the other mode, $v_{6,33}$, has a much weaker centrality dependence. The relatively large magnitude of these flow modes imply strong contributions from the second and third order harmonics. Finally, $v_{6,24}$ follows the trend of the total magnitude. The magnitude of $v_{6,24}$ comes close to the total, which in turn suggests not only strong contributions from the second harmonic order, but also the fourth one. The $v_{6,24}$ induced by the fourth order is seen to be the dominant contribution to the sixth order from 10% centrality classes and higher. For the seventh order v_7, there are three non-linear contributions, of which $v_{7,223}$ is measured. The centrality dependence is similar as with the v_6 coefficient, and there is a similar general trend as for the lower order harmonics among the non-linear flow modes.

The coefficients $\rho_{n,mk}$, quantifying the correlations amongst different symmetry planes, are presented as a function of centrality in figure 5. Except for $\rho_{6,33}$, all coefficients indicate an increase in correlation between symmetry planes with increasing centrality class of the collision. The measurements generally agree with the ones obtained at the lower energy. The $\rho_{6,222}$ is the only coefficient for which an energy dependence can be observed. The hydrodynamic calculations reproduce the measurements within the large theoretical uncertainties. For $\rho_{4,22}$, $\rho_{5,23}$, and $\rho_{6,222}$, TRENTo+param3 however underestimates the data in mid-central collisions.

Finally, the non-linear flow mode coefficients are presented in figure 6. Six coefficients are measured, of which four are compared with the lower beam energy results available
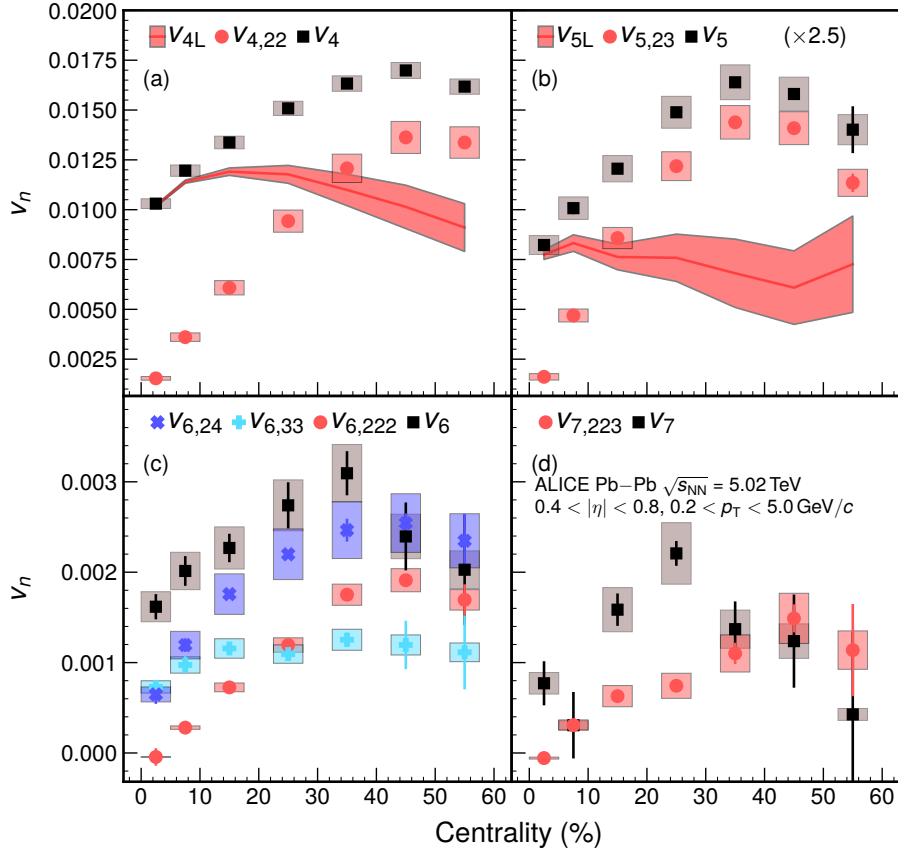
Figure 4. Linear and non-linear flow modes as a function of centrality. The total contribution measured in Pb-Pb collisions at $\sqrt{s_{NN}} = 5.02\,\text{TeV}$ is shown as black squares. Various non-linear contributions are presented in different red and blue colors, while the linear part, extracted from the aforementioned contributions, is shown as a red band. For panel (b), the data points are scaled by 2.5 for better visibility across the panels.

in [53]. For $\chi_{4,22}$ and $\chi_{5,23}$, the centrality dependence and overall magnitude agree well with the results from the lower beam energy. The centrality dependence of the new data is similar to the previous results: a larger value in more central collisions, decreasing close to unity towards 50% centrality.

All of the non-linear flow mode coefficients for the sixth harmonic agree with the previous measurements. The centrality dependence of $\chi_{6,222}$ is similar to the ones of the lower order coefficients, and the overall magnitude similar to $\chi_{4,22}$. As for $\chi_{6,33}$, no clear centrality dependence is observed within the current experimental uncertainties. Whereas the previous measurements are unable to distinguish between the magnitudes of $\chi_{6,222}$ and $\chi_{6,33}$, the current results show that $\chi_{6,222} > \chi_{6,33}$ across the whole centrality interval. For $\chi_{7,223}$, the overall magnitude is larger than for the other non-linear flow mode coefficients.

The hydrodynamic calculations for the non-linear flow mode coefficients show slightly more variation compared to the symmetry-plane correlations. As seen from the panels of figure 6, one observes the reproduction of the data points by EKRT+param0 up to
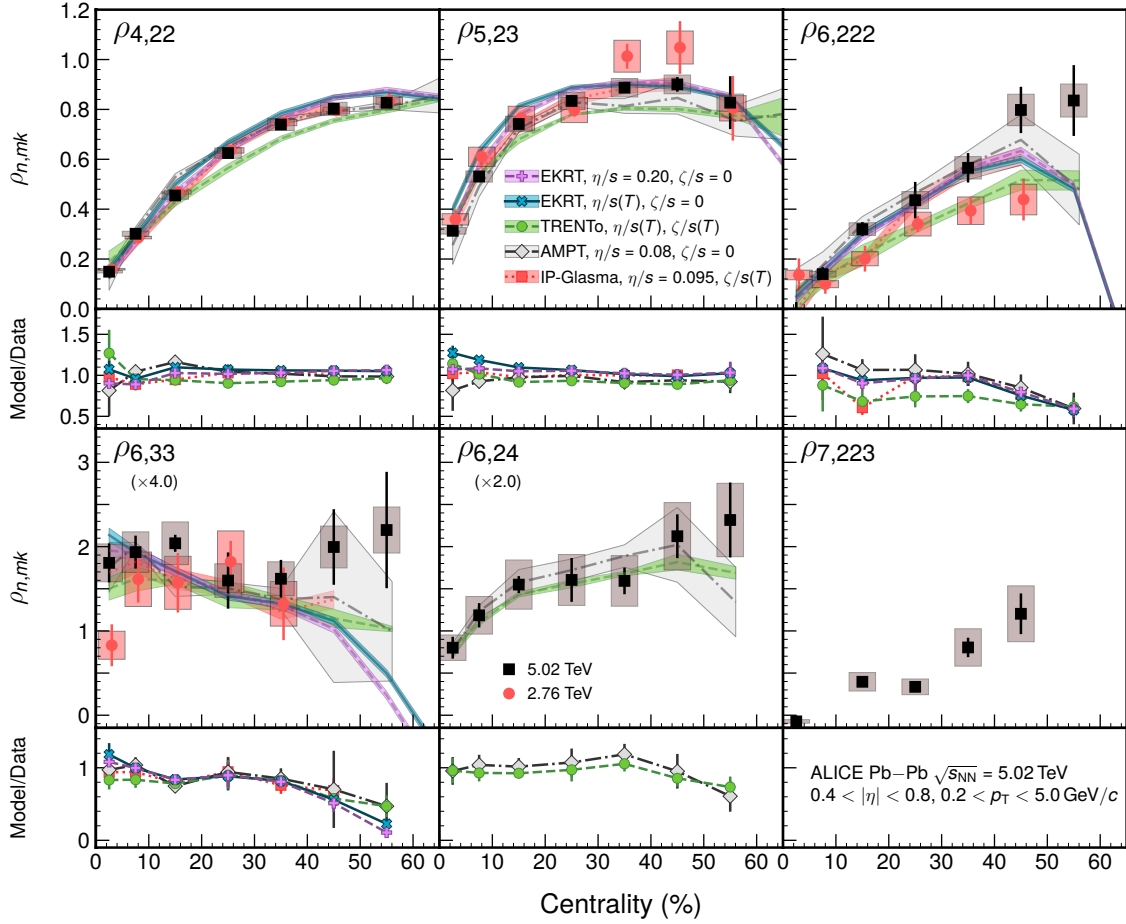
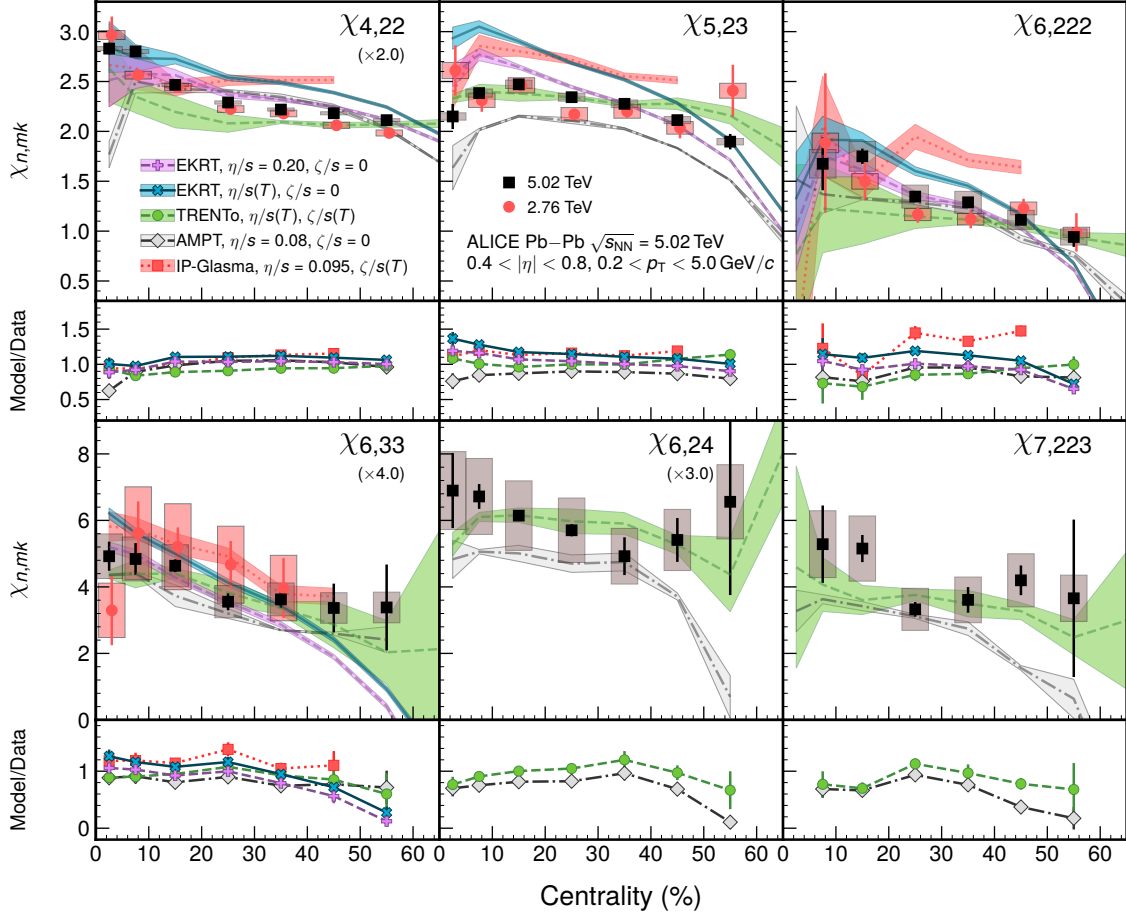**Figure 5**. Symmetry-plane correlations as a function of centrality in Pb-Pb collisions at $\sqrt{s_{\rm NN}} = 5.02$ TeV (black markers) compared with those in Pb-Pb collisions at $\sqrt{s_{\rm NN}} = 2.76$ TeV [53], along with five different hydrodynamic calculations shown as color bands. On the bottom part of each panel, the ratios between model calculations and the data are shown. For some panels, the data points are scaled by an indicated factor for better visibility.

the modes of the sixth harmonic, and T$_R$ENTo+param3 in all harmonics. The EKRT+ param1 calculations slightly overestimate the centrality dependence of the non-linear flow mode coefficients. It can be seen that the parameterizations of the EKRT presented here imply $\chi_{n,mk}$ across all harmonic orders to have sensitivity to η/s, whereas in the previous calculations in [53], weak η/s dependence was found for $\chi_{4,22}$ and $\chi_{6,222}$. The fifth order coefficient $\chi_{5,23}$ is expected to be quite sensitive to η/s in central collisions as can be seen from the difference of the predicted values from EKRT+param0 and EKRT+param1. The AMPT+param2 calculations underestimate the magnitude of some of the measured non-linear flow mode coefficients in various centrality classes, especially $\chi_{5,23}$, $\chi_{7,223}$ as well as $\chi_{6,24}$. The IP-Glasma+param4 calculations overestimate the measurements in some centrality intervals.

Figure 6. Non-linear mode coefficients as a function of centrality in Pb-Pb collisions at $\sqrt{s_{\mathrm{NN}}} = 5.02 \, \mathrm{TeV}$ (black markers) compared with those from $\sqrt{s_{\mathrm{NN}}} = 2.76 \, \mathrm{TeV}$ (red markers) [53], along with five different hydrodynamic calculations shown as color bands. On the bottom part of each panel, the ratios between model calculations and the data are shown. For some panels, the points are scaled by an indicated factor for better visibility across the panels.

The agreement between data and the model calculations is quantified by calculating the reduced χ^2/N_{dof} defined as

$$\chi^2/N_{\mathrm{dof}} = \frac{1}{N_{\mathrm{dof}}} \sum_{i=1}^{N_{\mathrm{dof}}} \frac{(y_i - f_i)^2}{\sigma_i^2}, \tag{5.1}$$

where y_i and f_i are the values for data and calculations, respectively, and $\sigma_i^2 = \sigma_{i,\mathrm{stat}}^2 + \sigma_{i,\mathrm{syst}}^2 + \sigma_{f_i,\mathrm{stat}}^2$ is the quadratic uncertainty in terms of statistical measurement $\sigma_{i,\mathrm{stat}}$, model uncertainties $\sigma_{f_i,\mathrm{stat}}$, and systematic uncertainties $\sigma_{i,\mathrm{syst}}$ in centrality bin i. Here N_{dof} represents the number of data points across the centrality interval.

The χ^2/N_{dof} for the flow coefficients are presented in figure 7, panel (a). It is observed that IP-Glasma+param4 gives the best description of v_2 and v_3 compared to the other models, indicated by the overall low value of χ^2/N_{dof}. However, the overall performance
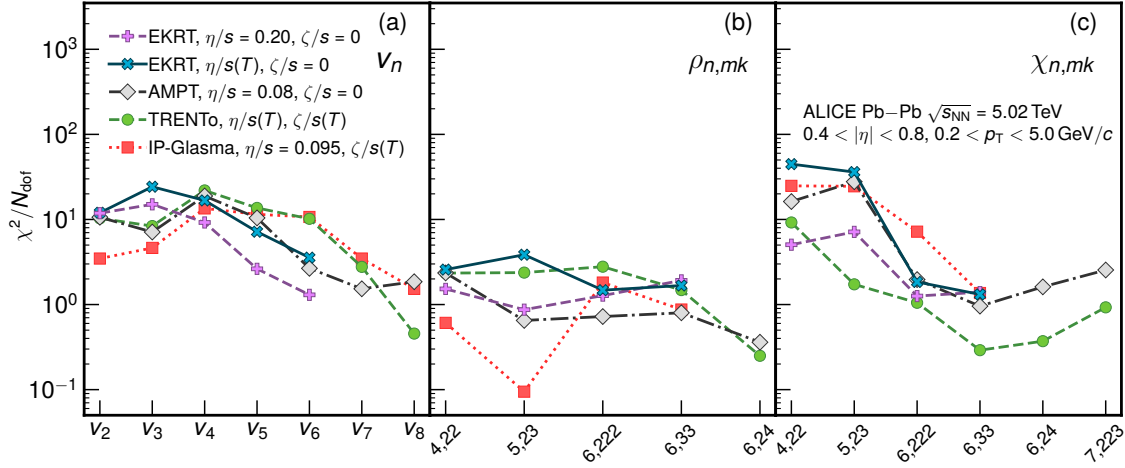
Figure 7. Overview of various model comparisons with data, quantified by χ^2/N_{dof}. Lower χ^2/N_{dof} represents a better overall description for a given observable.

of IP-Glasma+param4 is considerably worse at $n \geq 4$, for which the data are overestimated, as seen in figure 2. For v_4 to v_6, EKRT+param0 gives the lowest value of χ^2/N_{dof}. In the case of EKRT+param1, the χ^2/N_{dof} is slightly worse than EKRT+param0. The χ^2/N_{dof} of T$_R$ENTo+param3 is very close to that of IP-Glasma+param4, indicating a comparable description of data between the two model configurations. At low harmonic orders, T$_R$ENTo+param3 performs slightly worse than IP-Glasma+param4. For $n \geq 4$, description of the data between these two models are comparable except for $n = 8$, where T$_R$ENTo+param3 clearly has a better magnitude and centrality depiction. Notably this can be seen for v_8 where the χ^2/N_{dof} value is the lowest across all models. Finally, the performance of AMPT+param2 can be considered good within the reported χ^2/N_{dof} values. It is noted that the magnitude of v_7 is best depicted by AMPT+param2 amongst the three models used.

The performance of the models with respect to the symmetry-plane correlations is quantified in panel (b) of figure 7. IP-Glasma+param4 has by far the best estimates of $\rho_{n,mk}$ for $\rho_{4,22}$ and $\rho_{5,23}$. For other models, the model depiction is comparable. In low harmonic orders, EKRT+param0 shows good agreement with the data, as well as AMPT+ param2, which has the best agreement in higher harmonic orders. For T$_R$ENTo+param3, the agreement is slightly worse for $\rho_{5,23}$ and $\rho_{6,222}$.

The panel (c) of figure 7 shows the χ^2/N_{dof} for non-linear flow mode coefficients. As seen also in figure 6, T$_R$ENTo+param3 consistently provides the most successful overall description of the data. For other models the data are more frequently over- or underestimated. T$_R$ENTo+param3 estimates $\chi_{n,mk}$ better than it does the v_n coefficients, for which significant overestimation was present at almost every harmonic order (see figure 2). For EKRT+param0 the agreement is good, but the calculation over- or underestimates in some cases especially in most central or mid-peripheral collisions. Most of the observables are better described by the calculations using EKRT+param0 with a const $\eta/s = 0.2$ as compared to results from EKRT+param1 which uses a temperature dependent η/s value.

AMPT+param2 performs worse for low-order harmonics as it overpredicts the data in central and mid-central collisions. Of the five configurations, IP-Glasma+param4 describes the data worse in all harmonic orders.

The deviation of the calculated results from the measured value of each observable is of the same order of magnitude for the different models. Even where the model results show gross agreement with overall features in data, the values of $\chi^2/N_{\rm dof}$ vary considerably from one harmonic order to another. Considering the $\chi^2/N_{\rm dof}$ to be a goodness-of-fit estimate to validate any model, these variations suggest that the sensitivity of the different observables on the initial conditions, η/s, and ζ/s are reflected differently in the model calculations. Since the current uncertainties in the model calculations are large for higher order harmonics, the absolute χ^2 test should not be over-interpreted. Both, improved statistical uncertainties in the model calculations and different values of input parameters would be beneficial. However, large sets of calculations in many parameter spaces require substantial computing power. In order to constrain the model parameters Bayesian analysis can provide a plausible approach as demonstrated in [45, 47]. At present it is limited to low harmonic-order observables, and the extracted parameters have large uncertainties. Extending the Bayesian analysis to include the results in this paper will help reduce the uncertainties of the model parameters.

6 Summary

The measurements of anisotropic flow coefficients (v_n), non-linear flow mode coefficients ($\chi_{n,mk}$), and correlations among different symmetry planes ($\rho_{n,mk}$) in Pb-Pb collisions at $\sqrt{s_{\rm NN}} = 5.02\,{\rm TeV}$ are presented. The anisotropic flow coefficients are measured up to v_9, where v_8 and v_9 are measured for the first time at LHC energies. It is observed that v_n decreases as n increases, observing n-ordered damping up to $n = 7$. The v_n is found to be enhanced for $n > 7$. The non-linear contribution becomes dominant towards peripheral collisions in all harmonic orders. The strength of the non-linear flow mode and the symmetry-plane correlations depends also on harmonic orders. The non-linear flow mode coefficients show a clear centrality and harmonic order dependencies and the strongest non-linear mode coefficients is observed for the fifth and seventh harmonic orders.

These results are compared with various hydrodynamic model calculations with different initial conditions, as well as different parameterizations of η/s and ζ/s. None of the models presented in this paper simultaneously describe the v_n coefficients, $\chi_{n,mk}$, or $\rho_{n,mk}$. Based on the model and data comparisons, among all the models, the event-by-event viscous hydrodynamic model with EKRT initial conditions and a constant $\eta/s = 0.2$ is observed to describe the data best, as far as the harmonics up to the sixth order are concerned. As a result further tuning is required to find the accurate parameterization of η/s and ζ/s. It is found that the different order harmonic observables presented in this paper have different sensitivities to the initial conditions and the system properties. These results allow further model parameters to be optimized and the initial conditions and the transport properties of nuclear matter in ultra-relativistic heavy-ion collisions to be better constrained.

Acknowledgments

A List of observables

In this section the complete list of the measured observables is presented. By root-mean-squaring the equations in eq. (1.3), one obtains a starting point for the definitions presented in this section. Provided that the linear and non-linear parts are uncorrelated, the following harmonic projections are obtained

$$v_{4,22} = \frac{\Re\langle V_4 (V_2^*)^2\rangle}{\sqrt{\langle |V_2|^4\rangle}} \qquad v_{5,23} = \frac{\Re\langle V_5 V_2^* V_3^*\rangle}{\sqrt{\langle |V_2|^2 |V_3|^2\rangle}}$$
$$\approx \langle v_4 \cos(4\psi_4 - 4\psi_2)\rangle, \qquad \approx \langle v_5 \cos(5\psi_5 - 3\psi_3 - 2\psi_2)\rangle,$$
$$v_{6,222} = \frac{\Re\langle V_6 (V_2^*)^3\rangle}{\sqrt{\langle |V_2|^6\rangle}} \qquad v_{6,24} = \frac{\Re\langle V_6 V_2^* V_4^*\rangle}{\sqrt{\langle |V_2|^2 |V_4|^2\rangle}}$$
$$\approx \langle v_6 \cos(6\psi_6 - 6\psi_2)\rangle, \qquad \approx \langle v_6 \cos(6\psi_6 - 4\psi_4 - 2\psi_2)\rangle,$$
$$v_{6,33} = \frac{\Re\langle V_6 (V_3^*)^2\rangle}{\sqrt{\langle |V_3|^4\rangle}} \qquad v_{7,223} = \frac{\Re\langle V_7 (V_2^*)^2 V_3^*\rangle}{\sqrt{\langle |V_2|^4 |V_3|^2\rangle}} \tag{A.1}$$
$$\approx \langle v_6 \cos(6\psi_6 - 6\psi_3)\rangle, \qquad \approx \langle v_7 \cos(7\psi_7 - 4\psi_2 - 3\psi_3)\rangle,$$
$$v_{8,233} = \frac{\Re\langle V_8 V_2^* (V_3^*)^2\rangle}{\sqrt{\langle |V_2|^2 |V_3|^4\rangle}}$$
$$\approx \langle v_8 \cos(8\psi_8 - 2\psi_2 - 6\psi_3)\rangle,$$

with $v_{4,22}^2 = \chi_{4,22}^2 \langle |V_2|^4\rangle$, $v_{5,23}^2 = \chi_{5,23}^2 \langle |V_2|^2 |V_3|^2\rangle$, ... The rest of the observables we define using the harmonic projections in eq. (A.1). The symmetry plane correlations are defined as

$$\rho_{4,22} = \frac{v_{4,22}}{v_4}, \qquad \rho_{5,23} = \frac{v_{5,23}}{v_5},$$
$$\rho_{6,222} = \frac{v_{6,222}}{v_6}, \qquad \rho_{7,223} = \frac{v_{7,334}}{v_7}, \tag{A.2}$$
$$\rho_{6,33} = \frac{v_{6,33}}{v_6},$$

and the non-linear mode coefficients

$$\chi_{4,22} = \frac{v_{4,22}}{\sqrt{\langle v_2^4\rangle}}, \qquad \chi_{5,23} = \frac{v_{5,23}}{\sqrt{\langle v_2^2 v_3^2\rangle}},$$
$$\chi_{6,222} = \frac{v_{6,222}}{\sqrt{\langle v_2^6\rangle}}, \qquad \chi_{7,223} = \frac{v_{7,223}}{\sqrt{\langle v_2^4 v_3^2\rangle}},$$
$$\chi_{6,33} = \frac{v_{6,33}}{\sqrt{\langle v_3^4\rangle}}, \qquad\qquad\qquad\qquad \text{(A.3)}$$
$$\chi_{6,24} = \Re\frac{\langle V_6 V_2^* V_4^*\rangle\langle v_2^4\rangle - \langle V_6 (V_2^*)^3\rangle\langle V_4 (V_2^*)^2\rangle}{(\langle v_4^2\rangle\langle v_2^4\rangle - \langle V_4 (V_2^*)^2\rangle^2)\langle v_2^2\rangle}.$$

The higher order superpositions in eq. (1.3) include the coupling constants for the higher order linear responses. In a more complete treatment [100], the extraction of the higher order non-linear flow mode coefficients are performed by correlating the corresponding superpositions with those of the relevant harmonics, effectively resulting in a more general projection. The results agree with the expressions in eq. (2.4), and generate additional high order linear coupling coefficients

$$\chi_{6,24} = \Re\frac{\langle V_6 V_2^* V_4^*\rangle\langle v_2^4\rangle - \langle V_6 (V_2^*)^3\rangle\langle V_4 (V_2^*)^2\rangle}{(\langle v_4^2\rangle\langle v_2^4\rangle - \langle V_4 (V_2^*)^2\rangle^2)\langle v_2^2\rangle},$$
$$\chi_{7,25} = \Re\frac{\langle V_7 V_2^* V_5^*\rangle\langle v_2^2 v_3^2\rangle - \langle V_7 (V_2^*)^2 V_3^*\rangle\langle V_5 V_2^* V_3^*\rangle}{(\langle v_5^2\rangle\langle v_2^2 v_3^2\rangle - \langle V_5 V_2^* V_3^*\rangle^2)\langle v_2^2\rangle}, \qquad \text{(A.4)}$$
$$\chi_{7,34} = \Re\frac{\langle V_7 V_3^* V_4^*\rangle\langle v_2^4\rangle - \langle V_7 (V_2^*)^2 V_3^*\rangle\langle V_4 (V_2^*)^2\rangle}{(\langle v_4^2\rangle\langle v_2^4\rangle - \langle V_4 (V_2^*)^2\rangle^2)\langle v_3^2\rangle}.$$

Open Access. This article is distributed under the terms of the Creative Commons Attribution License (CC-BY 4.0), which permits any use, distribution and reproduction in any medium, provided the original author(s) and source are credited.

References

[1] J.-Y. Ollitrault, *Anisotropy as a signature of transverse collective flow*, *Phys. Rev.* **D 46** (1992) 229 [INSPIRE].

[2] S.A. Voloshin, A.M. Poskanzer and R. Snellings, *Collective phenomena in non-central nuclear collisions*, *Landolt-Bornstein* **23** (2010) 293 [arXiv:0809.2949] [INSPIRE].

[3] S. Voloshin and Y. Zhang, *Flow study in relativistic nuclear collisions by Fourier expansion of Azimuthal particle distributions*, *Z. Phys.* **C 70** (1996) 665 [hep-ph/9407282] [INSPIRE].

[4] A.M. Poskanzer and S.A. Voloshin, *Methods for analyzing anisotropic flow in relativistic nuclear collisions*, *Phys. Rev.* **C 58** (1998) 1671 [nucl-ex/9805001] [INSPIRE].

[5] B. Alver and G. Roland, *Collision geometry fluctuations and triangular flow in heavy-ion collisions*, *Phys. Rev.* **C 81** (2010) 054905 [*Erratum ibid.* **C 82** (2010) 039903] [arXiv:1003.0194] [INSPIRE].

[6] ALICE collaboration, *Higher harmonic anisotropic flow measurements of charged particles in Pb-Pb collisions at $\sqrt{s_{NN}} = 2.76$ TeV*, *Phys. Rev. Lett.* **107** (2011) 032301 [arXiv:1105.3865] [INSPIRE].

[7] ALICE collaboration, *Elliptic flow of charged particles in Pb-Pb collisions at* 2.76 *TeV*, *Phys. Rev. Lett.* **105** (2010) 252302 [arXiv:1011.3914] [InSPIRE].

[8] ALICE collaboration, *Anisotropic flow of charged hadrons, pions and (anti-)protons measured at high transverse momentum in Pb-Pb collisions at* $\sqrt{s_{NN}} = 2.76$ *TeV*, *Phys. Lett.* **B 719** (2013) 18 [arXiv:1205.5761] [InSPIRE].

[9] ALICE collaboration, *Elliptic flow of identified hadrons in Pb-Pb collisions at* $\sqrt{s_{NN}} = 2.76$ *TeV*, *JHEP* **06** (2015) 190 [arXiv:1405.4632] [InSPIRE].

[10] ALICE collaboration, *Higher harmonic flow coefficients of identified hadrons in Pb-Pb collisions at* $\sqrt{s_{NN}} = 2.76$ *TeV*, *JHEP* **09** (2016) 164 [arXiv:1606.06057] [InSPIRE].

[11] ALICE collaboration, *Anisotropic flow of charged particles in Pb-Pb collisions at* $\sqrt{s_{NN}} = 5.02$ *TeV*, *Phys. Rev. Lett.* **116** (2016) 132302 [arXiv:1602.01119] [InSPIRE].

[12] ALICE collaboration, *Searches for transverse momentum dependent flow vector fluctuations in Pb-Pb and p-Pb collisions at the LHC*, *JHEP* **09** (2017) 032 [arXiv:1707.05690] [InSPIRE].

[13] ALICE collaboration, *Anisotropic flow of identified particles in Pb-Pb collisions at* $\sqrt{s_{NN}} = 5.02$ *TeV*, *JHEP* **09** (2018) 006 [arXiv:1805.04390] [InSPIRE].

[14] D.A. Teaney, *Viscous Hydrodynamics and the Quark Gluon Plasma*, in *Quark-gluon plasma 4*, R.C. Hwa and X.-N. Wang eds., pp. 207–266, (2010) [DOI] [arXiv:0905.2433] [InSPIRE].

[15] D. Molnar and M. Gyulassy, *Saturation of elliptic flow and the transport opacity of the gluon plasma at RHIC*, *Nucl. Phys.* **A 697** (2002) 495 [*Erratum ibid.* **A 703** (2002) 893] [nucl-th/0104073] [InSPIRE].

[16] D. Teaney, *The Effects of viscosity on spectra, elliptic flow and HBT radii*, *Phys. Rev.* **C 68** (2003) 034913 [nucl-th/0301099] [InSPIRE].

[17] R.A. Lacey et al., *Has the QCD Critical Point been Signaled by Observations at RHIC?*, *Phys. Rev. Lett.* **98** (2007) 092301 [nucl-ex/0609025] [InSPIRE].

[18] H.-J. Drescher, A. Dumitru, C. Gombeaud and J.-Y. Ollitrault, *The Centrality dependence of elliptic flow, the hydrodynamic limit and the viscosity of hot QCD*, *Phys. Rev.* **C 76** (2007) 024905 [arXiv:0704.3553] [InSPIRE].

[19] Z. Xu, C. Greiner and H. Stocker, *PQCD calculations of elliptic flow and shear viscosity at RHIC*, *Phys. Rev. Lett.* **101** (2008) 082302 [arXiv:0711.0961] [InSPIRE].

[20] D. Molnar and P. Huovinen, *Dissipative effects from transport and viscous hydrodynamics*, *J. Phys.* **G 35** (2008) 104125 [arXiv:0806.1367] [InSPIRE].

[21] U. Heinz and R. Snellings, *Collective flow and viscosity in relativistic heavy-ion collisions*, *Ann. Rev. Nucl. Part. Sci.* **63** (2013) 123 [arXiv:1301.2826] [InSPIRE].

[22] H. Song, Y. Zhou and K. Gajdosova, *Collective flow and hydrodynamics in large and small systems at the LHC*, *Nucl. Sci. Tech.* **28** (2017) 99 [arXiv:1703.00670] [InSPIRE].

[23] P. Kovtun, D.T. Son and A.O. Starinets, *Viscosity in strongly interacting quantum field theories from black hole physics*, *Phys. Rev. Lett.* **94** (2005) 111601 [hep-th/0405231] [InSPIRE].

[24] D. Teaney and L. Yan, *Triangularity and Dipole Asymmetry in Heavy Ion Collisions*, *Phys. Rev.* **C 83** (2011) 064904 [arXiv:1010.1876] [InSPIRE].

[25] H. Niemi, K.J. Eskola and R. Paatelainen, *Event-by-event fluctuations in a perturbative QCD + saturation + hydrodynamics model: Determining QCD matter shear viscosity in ultrarelativistic heavy-ion collisions*, *Phys. Rev.* **C 93** (2016) 024907 [arXiv:1505.02677] [INSPIRE].

[26] H. Niemi, G.S. Denicol, H. Holopainen and P. Huovinen, *Event-by-event distributions of azimuthal asymmetries in ultrarelativistic heavy-ion collisions*, *Phys. Rev.* **C 87** (2013) 054901 [arXiv:1212.1008] [INSPIRE].

[27] STAR collaboration, *Identified particle elliptic flow in Au + Au collisions at $\sqrt{s_{NN}} = 130\,GeV$*, *Phys. Rev. Lett.* **87** (2001) 182301 [nucl-ex/0107003] [INSPIRE].

[28] STAR collaboration, *Elliptic flow from two and four particle correlations in Au+Au collisions at $\sqrt{s_{NN}} = 130\,GeV$*, *Phys. Rev.* **C 66** (2002) 034904 [nucl-ex/0206001] [INSPIRE].

[29] PHENIX collaboration, *Elliptic flow of identified hadrons in Au+Au collisions at $\sqrt{s_{NN}} = 200\,GeV$*, *Phys. Rev. Lett.* **91** (2003) 182301 [nucl-ex/0305013] [INSPIRE].

[30] STAR collaboration, *Azimuthal anisotropy at RHIC: The First and fourth harmonics*, *Phys. Rev. Lett.* **92** (2004) 062301 [nucl-ex/0310029] [INSPIRE].

[31] STAR collaboration, *Azimuthal anisotropy in U+U and Au+Au collisions at RHIC*, *Phys. Rev. Lett.* **115** (2015) 222301 [arXiv:1505.07812] [INSPIRE].

[32] PHOBOS collaboration, *Event-by-Event Fluctuations of Azimuthal Particle Anisotropy in Au + Au Collisions at $\sqrt{s_{NN}} = 200\,GeV$*, *Phys. Rev. Lett.* **104** (2010) 142301 [nucl-ex/0702036] [INSPIRE].

[33] T. Hirano, U.W. Heinz, D. Kharzeev, R. Lacey and Y. Nara, *Hadronic dissipative effects on elliptic flow in ultrarelativistic heavy-ion collisions*, *Phys. Lett.* **B 636** (2006) 299 [nucl-th/0511046] [INSPIRE].

[34] P. Romatschke and U. Romatschke, *Viscosity Information from Relativistic Nuclear Collisions: How Perfect is the Fluid Observed at RHIC?*, *Phys. Rev. Lett.* **99** (2007) 172301 [arXiv:0706.1522] [INSPIRE].

[35] A.K. Chaudhuri, *Saturation of elliptic flow and shear viscosity*, arXiv:0708.1252 [INSPIRE].

[36] H. Song, S.A. Bass, U. Heinz, T. Hirano and C. Shen, *200 A GeV Au+Au collisions serve a nearly perfect quark-gluon liquid*, *Phys. Rev. Lett.* **106** (2011) 192301 [*Erratum ibid.* **109** (2012) 139904] [arXiv:1011.2783] [INSPIRE].

[37] M. Luzum and J.-Y. Ollitrault, *Extracting the shear viscosity of the quark-gluon plasma from flow in ultra-central heavy-ion collisions*, *Nucl. Phys.* **A904–905** (2013) 377c [arXiv:1210.6010] [INSPIRE].

[38] C. Shen et al., *The QGP shear viscosity: Elusive goal or just around the corner?*, *J. Phys.* **G 38** (2011) 124045 [arXiv:1106.6350] [INSPIRE].

[39] ALICE collaboration, *Correlated event-by-event fluctuations of flow harmonics in Pb-Pb collisions at $\sqrt{s_{NN}} = 2.76\,TeV$*, *Phys. Rev. Lett.* **117** (2016) 182301 [arXiv:1604.07663] [INSPIRE].

[40] ALICE collaboration, *Systematic studies of correlations between different order flow harmonics in Pb-Pb collisions at $\sqrt{s_{NN}} = 2.76\,TeV$*, *Phys. Rev.* **C 97** (2018) 024906 [arXiv:1709.01127] [INSPIRE].

[41] P. Bozek, *Flow and interferometry in 3+1 dimensional viscous hydrodynamics*, *Phys. Rev.* **C 85** (2012) 034901 [arXiv:1110.6742] [INSPIRE].

[42] J.-B. Rose et al., *Extracting the bulk viscosity of the quark-gluon plasma*, *Nucl. Phys.* **A 931** (2014) 926 [arXiv:1408.0024] [INSPIRE].

[43] S. Ryu et al., *Importance of the Bulk Viscosity of QCD in Ultrarelativistic Heavy-Ion Collisions*, *Phys. Rev. Lett.* **115** (2015) 132301 [arXiv:1502.01675] [INSPIRE].

[44] S. Ryu et al., *Effects of bulk viscosity and hadronic rescattering in heavy ion collisions at energies available at the BNL Relativistic Heavy Ion Collider and at the CERN Large Hadron Collider*, *Phys. Rev.* **C 97** (2018) 034910 [arXiv:1704.04216] [INSPIRE].

[45] J.E. Bernhard, J.S. Moreland, S.A. Bass, J. Liu and U. Heinz, *Applying Bayesian parameter estimation to relativistic heavy-ion collisions: simultaneous characterization of the initial state and quark-gluon plasma medium*, *Phys. Rev.* **C 94** (2016) 024907 [arXiv:1605.03954] [INSPIRE].

[46] A. Dubla, S. Masciocchi, J.M. Pawlowski, B. Schenke, C. Shen and J. Stachel, *Towards QCD-assisted hydrodynamics for heavy-ion collision phenomenology*, *Nucl. Phys.* **A 979** (2018) 251 [arXiv:1805.02985] [INSPIRE].

[47] J.E. Bernhard, J.S. Moreland and S.A. Bass, *Bayesian estimation of the specific shear and bulk viscosity of quark-gluon plasma*, *Nature Phys.* **15** (2019) 1113.

[48] B.H. Alver, C. Gombeaud, M. Luzum and J.-Y. Ollitrault, *Triangular flow in hydrodynamics and transport theory*, *Phys. Rev.* **C 82** (2010) 034913 [arXiv:1007.5469] [INSPIRE].

[49] ATLAS collaboration, *Measurement of the azimuthal anisotropy of charged particles produced in $\sqrt{s_{NN}} = 5.02\,TeV\,Pb+Pb$ collisions with the ATLAS detector*, *Eur. Phys. J.* **C 78** (2018) 997 [arXiv:1808.03951] [INSPIRE].

[50] F.G. Gardim, F. Grassi, M. Luzum and J.-Y. Ollitrault, *Mapping the hydrodynamic response to the initial geometry in heavy-ion collisions*, *Phys. Rev.* **C 85** (2012) 024908 [arXiv:1111.6538] [INSPIRE].

[51] F.G. Gardim, J. Noronha-Hostler, M. Luzum and F. Grassi, *Effects of viscosity on the mapping of initial to final state in heavy ion collisions*, *Phys. Rev.* **C 91** (2015) 034902 [arXiv:1411.2574] [INSPIRE].

[52] D. Teaney and L. Yan, *Event-plane correlations and hydrodynamic simulations of heavy ion collisions*, *Phys. Rev.* **C 90** (2014) 024902 [arXiv:1312.3689] [INSPIRE].

[53] ALICE collaboration, *Linear and non-linear flow modes in Pb-Pb collisions at $\sqrt{s_{NN}} = 2.76\,TeV$*, *Phys. Lett.* **B 773** (2017) 68 [arXiv:1705.04377] [INSPIRE].

[54] M.L. Miller, K. Reygers, S.J. Sanders and P. Steinberg, *Glauber modeling in high energy nuclear collisions*, *Ann. Rev. Nucl. Part. Sci.* **57** (2007) 205 [nucl-ex/0701025] [INSPIRE].

[55] Z. Qiu and U.W. Heinz, *Event-by-event shape and flow fluctuations of relativistic heavy-ion collision fireballs*, *Phys. Rev.* **C 84** (2011) 024911 [arXiv:1104.0650] [INSPIRE].

[56] H.-J. Drescher and Y. Nara, *Eccentricity fluctuations from the color glass condensate at RHIC and LHC*, *Phys. Rev.* **C 76** (2007) 041903 [arXiv:0707.0249] [INSPIRE].

[57] S. McDonald, C. Shen, F. Fillion-Gourdeau, S. Jeon and C. Gale, *Hydrodynamic predictions for Pb+Pb collisions at 5.02 TeV*, *Phys. Rev.* **C 95** (2017) 064913 [arXiv:1609.02958] [INSPIRE].

[58] ALICE collaboration, *Energy dependence and fluctuations of anisotropic flow in Pb-Pb collisions at* $\sqrt{s_{\mathrm{NN}}} = 5.02$ *and* 2.76 *TeV*, *JHEP* **07** (2018) 103 [arXiv:1804.02944] [INSPIRE].

[59] L. Yan and J.-Y. Ollitrault, $\nu_4, \nu_5, \nu_6, \nu_7$: *nonlinear hydrodynamic response versus LHC data*, *Phys. Lett.* **B 744** (2015) 82 [arXiv:1502.02502] [INSPIRE].

[60] D. Teaney and L. Yan, *Non linearities in the harmonic spectrum of heavy ion collisions with ideal and viscous hydrodynamics*, *Phys. Rev.* **C 86** (2012) 044908 [arXiv:1206.1905] [INSPIRE].

[61] J. Jia and S. Mohapatra, *A Method for studying initial geometry fluctuations via event plane correlations in heavy ion collisions*, *Eur. Phys. J.* **C 73** (2013) 2510 [arXiv:1203.5095] [INSPIRE].

[62] M. Luzum, *Flow fluctuations and long-range correlations: elliptic flow and beyond*, *J. Phys.* **G 38** (2011) 124026 [arXiv:1107.0592] [INSPIRE].

[63] Z. Qiu and U. Heinz, *Hydrodynamic event-plane correlations in Pb+Pb collisions at* $\sqrt{s} = 2.76ATeV$, *Phys. Lett.* **B 717** (2012) 261 [arXiv:1208.1200] [INSPIRE].

[64] ATLAS collaboration, *Measurement of event-plane correlations in* $\sqrt{s_{NN}} = 2.76$ *TeV lead-lead collisions with the ATLAS detector*, *Phys. Rev.* **C 90** (2014) 024905 [arXiv:1403.0489] [INSPIRE].

[65] CMS collaboration, *Measurement of Higher-Order Harmonic Azimuthal Anisotropy in PbPb Collisions at* $\sqrt{s_{NN}} = 2.76$ *TeV*, *Phys. Rev.* **C 89** (2014) 044906 [arXiv:1310.8651] [INSPIRE].

[66] M. Luzum and J.-Y. Ollitrault, *Eliminating experimental bias in anisotropic-flow measurements of high-energy nuclear collisions*, *Phys. Rev.* **C 87** (2013) 044907 [arXiv:1209.2323] [INSPIRE].

[67] ALICE collaboration, *The ALICE experiment at the CERN LHC*, 2008 *JINST* **3** S08002 [INSPIRE].

[68] ALICE collaboration, *Performance of the ALICE Experiment at the CERN LHC*, *Int. J. Mod. Phys.* **A 29** (2014) 1430044 [arXiv:1402.4476] [INSPIRE].

[69] ALICE collaboration, *ALICE: Physics performance report, volume I*, *J. Phys.* **G 30** (2004) 1517 [INSPIRE].

[70] ALICE collaboration, *ALICE: Physics performance report, volume II*, *J. Phys.* **G 32** (2006) 1295 [INSPIRE].

[71] ALICE collaboration, *Performance of the ALICE VZERO system*, 2013 *JINST* **8** P10016 [arXiv:1306.3130] [INSPIRE].

[72] ALICE collaboration, *Alignment of the ALICE Inner Tracking System with cosmic-ray tracks*, 2010 *JINST* **5** P03003 [arXiv:1001.0502] [INSPIRE].

[73] ALICE collaboration, *Performance of the ALICE Time-Of-Flight detector at the LHC*, 2019 *JINST* **14** C06023 [arXiv:1806.03825] [INSPIRE].

[74] ALICE collaboration, *Centrality determination of Pb-Pb collisions at* $\sqrt{s_{NN}} = 2.76$ *TeV with ALICE*, *Phys. Rev.* **C 88** (2013) 044909 [arXiv:1301.4361] [INSPIRE].

[75] J. Alme et al., *The ALICE TPC, a large 3-dimensional tracking device with fast readout for ultra-high multiplicity events*, *Nucl. Instrum. Meth.* **A 622** (2010) 316 [arXiv:1001.1950] [INSPIRE].

[76] ALICE collaboration, *The ALICE definition of primary particles*, ALICE-PUBLIC-2017-005.

[77] X.-N. Wang and M. Gyulassy, *HIJING: A Monte Carlo model for multiple jet production in p p, p A and A A collisions*, *Phys. Rev.* **D 44** (1991) 3501 [INSPIRE].

[78] M. Gyulassy and X.-N. Wang, *HIJING 1.0: A Monte Carlo program for parton and particle production in high-energy hadronic and nuclear collisions*, *Comput. Phys. Commun.* **83** (1994) 307 [nucl-th/9502021] [INSPIRE].

[79] R. Brun et al., *GEANT Detector Description and Simulation Tool*, DOI [INSPIRE].

[80] A. Bilandzic, C.H. Christensen, K. Gulbrandsen, A. Hansen and Y. Zhou, *Generic framework for anisotropic flow analyses with multiparticle azimuthal correlations*, *Phys. Rev.* **C 89** (2014) 064904 [arXiv:1312.3572] [INSPIRE].

[81] H. Niemi, K.J. Eskola, R. Paatelainen and K. Tuominen, *Predictions for 5.023 TeV Pb + Pb collisions at the CERN Large Hadron Collider*, *Phys. Rev.* **C 93** (2016) 014912 [arXiv:1511.04296] [INSPIRE].

[82] W. Zhao, H.-j. Xu and H. Song, *Collective flow in 2.76 and 5.02 A TeV Pb+Pb collisions*, *Eur. Phys. J.* **C 77** (2017) 645 [arXiv:1703.10792] [INSPIRE].

[83] C. Shen, Z. Qiu, H. Song, J. Bernhard, S. Bass and U. Heinz, *The iEBE-VISHNU code package for relativistic heavy-ion collisions*, *Comput. Phys. Commun.* **199** (2016) 61 [arXiv:1409.8164] [INSPIRE].

[84] R.S. Bhalerao, A. Jaiswal and S. Pal, *Collective flow in event-by-event partonic transport plus hydrodynamics hybrid approach*, *Phys. Rev.* **C 92** (2015) 014903 [arXiv:1503.03862] [INSPIRE].

[85] L. Pang, Q. Wang and X.-N. Wang, *Effects of initial flow velocity fluctuation in event-by-event (3+1)D hydrodynamics*, *Phys. Rev.* **C 86** (2012) 024911 [arXiv:1205.5019] [INSPIRE].

[86] H.-j. Xu, Z. Li and H. Song, *High-order flow harmonics of identified hadrons in 2.76A TeV Pb + Pb collisions*, *Phys. Rev.* **C 93** (2016) 064905 [arXiv:1602.02029] [INSPIRE].

[87] J.S. Moreland, J.E. Bernhard and S.A. Bass, *Alternative ansatz to wounded nucleon and binary collision scaling in high-energy nuclear collisions*, *Phys. Rev.* **C 92** (2015) 011901 [arXiv:1412.4708] [INSPIRE].

[88] B. Schenke, S. Jeon and C. Gale, *Elliptic and triangular flow in event-by-event (3+1)D viscous hydrodynamics*, *Phys. Rev. Lett.* **106** (2011) 042301 [arXiv:1009.3244] [INSPIRE].

[89] B. Schenke, P. Tribedy and R. Venugopalan, *Fluctuating Glasma initial conditions and flow in heavy ion collisions*, *Phys. Rev. Lett.* **108** (2012) 252301 [arXiv:1202.6646] [INSPIRE].

[90] Z. Qiu, C. Shen and U. Heinz, *Hydrodynamic elliptic and triangular flow in Pb-Pb collisions at $\sqrt{s} = 2.76ATeV$*, *Phys. Lett.* **B 707** (2012) 151 [arXiv:1110.3033] [INSPIRE].

[91] C. Shen, U. Heinz, P. Huovinen and H. Song, *Systematic parameter study of hadron spectra and elliptic flow from viscous hydrodynamic simulations of Au+Au collisions at $\sqrt{s_{NN}} = 200\,GeV$*, *Phys. Rev.* **C 82** (2010) 054904 [arXiv:1010.1856] [INSPIRE].

[92] C. Shen, U. Heinz, P. Huovinen and H. Song, *Radial and elliptic flow in Pb+Pb collisions at the Large Hadron Collider from viscous hydrodynamic*, *Phys. Rev.* **C 84** (2011) 044903 [arXiv:1105.3226] [INSPIRE].

[93] G.S. Denicol, T. Kodama, T. Koide and P. Mota, *Effect of bulk viscosity on Elliptic Flow near QCD phase transition*, *Phys. Rev.* **C 80** (2009) 064901 [`arXiv:0903.3595`] [INSPIRE].

[94] F. Karsch, D. Kharzeev and K. Tuchin, *Universal properties of bulk viscosity near the QCD phase transition*, *Phys. Lett.* **B 663** (2008) 217 [`arXiv:0711.0914`] [INSPIRE].

[95] J. Noronha-Hostler, J. Noronha and C. Greiner, *Transport Coefficients of Hadronic Matter near T(c)*, *Phys. Rev. Lett.* **103** (2009) 172302 [`arXiv:0811.1571`] [INSPIRE].

[96] E. Molnar, H. Niemi and D.H. Rischke, *Numerical tests of causal relativistic dissipative fluid dynamics*, *Eur. Phys. J.* **C 65** (2010) 615 [`arXiv:0907.2583`] [INSPIRE].

[97] E. Shuryak, *The sounds of the Little and Big Bangs*, *Universe* **3** (2017) 75 [`arXiv:1710.03776`] [INSPIRE].

[98] P. Staig and E. Shuryak, *The Fate of the Initial State Fluctuations in Heavy Ion Collisions. III The Second Act of Hydrodynamics*, *Phys. Rev.* **C 84** (2011) 044912 [`arXiv:1105.0676`] [INSPIRE].

[99] R.A. Lacey et al., *Is anisotropic flow really acoustic?*, `arXiv:1301.0165` [INSPIRE].

[100] J. Qian, U.W. Heinz and J. Liu, *Mode-coupling effects in anisotropic flow in heavy-ion collisions*, *Phys. Rev.* **C 93** (2016) 064901 [`arXiv:1602.02813`] [INSPIRE].

The ALICE collaboration

S. Acharya[141], D. Adamová[94], A. Adler[74], J. Adolfsson[80], M.M. Aggarwal[99], G. Aglieri Rinella[33],
M. Agnello[30], N. Agrawal[10,53], Z. Ahammed[141], S. Ahmad[16], S.U. Ahn[76], A. Akindinov[91],
M. Al-Turany[106], S.N. Alam[141], D.S.D. Albuquerque[122], D. Aleksandrov[87], B. Alessandro[58],
H.M. Alfanda[6], R. Alfaro Molina[71], B. Ali[16], Y. Ali[14], A. Alici[10,26,53], A. Alkin[2], J. Alme[21],
T. Alt[68], L. Altenkamper[21], I. Altsybeev[112], M.N. Anaam[6], C. Andrei[47], D. Andreou[33],
H.A. Andrews[110], A. Andronic[144], M. Angeletti[33], V. Anguelov[103], C. Anson[15], T. Antičić[107],
F. Antinori[56], P. Antonioli[53], N. Apadula[79], L. Aphecetche[114], H. Appelshäuser[68], S. Arcelli[26],
R. Arnaldi[58], M. Arratia[79], I.C. Arsene[20], M. Arslandok[103], A. Augustinus[33], R. Averbeck[106],
S. Aziz[61], M.D. Azmi[16], A. Badalà[55], Y.W. Baek[40], S. Bagnasco[58], X. Bai[106], R. Bailhache[68],
R. Bala[100], A. Balbino[30], A. Baldisseri[137], M. Ball[42], S. Balouza[104], R. Barbera[27], L. Barioglio[25],
G.G. Barnaföldi[145], L.S. Barnby[93], V. Barret[134], P. Bartalini[6], K. Barth[33], E. Bartsch[68],
F. Baruffaldi[28], N. Bastid[134], S. Basu[143], G. Batigne[114], B. Batyunya[75], D. Bauri[48],
J.L. Bazo Alba[111], I.G. Bearden[88], C. Beattie[146], C. Bedda[63], N.K. Behera[60], I. Belikov[136],
A.D.C. Bell Hechavarria[144], F. Bellini[33], R. Bellwied[125], V. Belyaev[92], G. Bencedi[145], S. Beole[25],
A. Bercuci[47], Y. Berdnikov[97], D. Berenyi[145], R.A. Bertens[130], D. Berzano[58], M.G. Besoiu[67],
L. Betev[33], A. Bhasin[100], I.R. Bhat[100], M.A. Bhat[3], H. Bhatt[48], B. Bhattacharjee[41], A. Bianchi[25],
L. Bianchi[25], N. Bianchi[51], J. Bielčík[36], J. Bielčíková[94], A. Bilandzic[104,117], G. Biro[145],
R. Biswas[3], S. Biswas[3], J.T. Blair[119], D. Blau[87], C. Blume[68], G. Boca[139], F. Bock[33,95],
A. Bogdanov[92], L. Boldizsár[145], A. Bolozdynya[92], M. Bombara[37], G. Bonomi[140], H. Borel[137],
A. Borissov[92,144], H. Bossi[146], E. Botta[25], L. Bratrud[68], P. Braun-Munzinger[106], M. Bregant[121],
M. Broz[36], E. Bruna[58], G.E. Bruno[105], M.D. Buckland[127], D. Budnikov[108], H. Buesching[68],
S. Bufalino[30], O. Bugnon[114], P. Buhler[113], P. Buncic[33], Z. Buthelezi[72,131], J.B. Butt[14],
J.T. Buxton[96], S.A. Bysiak[118], D. Caffarri[89], A. Caliva[106], E. Calvo Villar[111], R.S. Camacho[44],
P. Camerini[24], A.A. Capon[113], F. Carnesecchi[10,26], R. Caron[137], J. Castillo Castellanos[137],
A.J. Castro[130], E.A.R. Casula[54], F. Catalano[30], C. Ceballos Sanchez[52], P. Chakraborty[48],
S. Chandra[141], W. Chang[6], S. Chapeland[33], M. Chartier[127], S. Chattopadhyay[141],
S. Chattopadhyay[109], A. Chauvin[23], C. Cheshkov[135], B. Cheynis[135], V. Chibante Barroso[33],
D.D. Chinellato[122], S. Cho[60], P. Chochula[33], T. Chowdhury[134], P. Christakoglou[89],
C.H. Christensen[88], P. Christiansen[80], T. Chujo[133], C. Cicalo[54], L. Cifarelli[10,26], F. Cindolo[53],
G. Clai[53, ii], J. Cleymans[124], F. Colamaria[52], D. Colella[52], A. Collu[79], M. Colocci[26],
M. Concas[58, iii], G. Conesa Balbastre[78], Z. Conesa del Valle[61], G. Contin[24,127], J.G. Contreras[36],
T.M. Cormier[95], Y. Corrales Morales[25], P. Cortese[31], M.R. Cosentino[123], F. Costa[33],
S. Costanza[139], P. Crochet[134], E. Cuautle[69], P. Cui[6], L. Cunqueiro[95], D. Dabrowski[142],
T. Dahms[104,117], A. Dainese[56], F.P.A. Damas[114,137], M.C. Danisch[103], A. Danu[67], D. Das[109],
I. Das[109], P. Das[85], P. Das[3], S. Das[3], A. Dash[85], S. Dash[48], S. De[85], A. De Caro[29], G. de
Cataldo[52], J. de Cuveland[38], A. De Falco[23], D. De Gruttola[10], N. De Marco[58], S. De Pasquale[29],
S. Deb[49], B. Debjani[3], H.F. Degenhardt[121], K.R. Deja[142], A. Deloff[84], S. Delsanto[25,131],
W. Deng[6], D. Devetak[106], P. Dhankher[48], D. Di Bari[32], A. Di Mauro[33], R.A. Diaz[8], T. Dietel[124],
P. Dillenseger[68], Y. Ding[6], R. Divià[33], D.U. Dixit[19], Ø. Djuvsland[21], U. Dmitrieva[62],
A. Dobrin[33,67], B. Dönigus[68], O. Dordic[20], A.K. Dubey[141], A. Dubla[106], S. Dudi[99],
M. Dukhishyam[85], P. Dupieux[134], R.J. Ehlers[95,146], V.N. Eikeland[21], D. Elia[52], E. Epple[146],
B. Erazmus[114], F. Erhardt[98], A. Erokhin[112], M.R. Ersdal[21], B. Espagnon[61], G. Eulisse[33],
D. Evans[110], S. Evdokimov[90], L. Fabbietti[104,117], M. Faggin[28], J. Faivre[78], F. Fan[6], A. Fantoni[51],
M. Fasel[95], P. Fecchio[30], A. Feliciello[58], G. Feofilov[112], A. Fernández Téllez[44], A. Ferrero[137],
A. Ferretti[25], A. Festanti[33], V.J.G. Feuillard[103], J. Figiel[118], S. Filchagin[108], D. Finogeev[62],
F.M. Fionda[21], G. Fiorenza[52], F. Flor[125], S. Foertsch[72], P. Foka[106], S. Fokin[87], E. Fragiacomo[59],

U. Frankenfeld[106], U. Fuchs[33], C. Furget[78], A. Furs[62], M. Fusco Girard[29], J.J. Gaardhøje[88],
M. Gagliardi[25], A.M. Gago[111], A. Gal[136], C.D. Galvan[120], P. Ganoti[83], C. Garabatos[106],
E. Garcia-Solis[11], K. Garg[27], C. Gargiulo[33], A. Garibli[86], K. Garner[144], P. Gasik[104,117],
E.F. Gauger[119], M.B. Gay Ducati[70], M. Germain[114], J. Ghosh[109], P. Ghosh[141], S.K. Ghosh[3],
M. Giacalone[26], P. Gianotti[51], P. Giubellino[58,106], P. Giubilato[28], P. Glässel[103], A. Gomez
Ramirez[74], V. Gonzalez[106], P. González-Zamora[44], S. Gorbunov[38], L. Görlich[118], S. Gotovac[34],
V. Grabski[71], L.K. Graczykowski[142], K.L. Graham[110], L. Greiner[79], A. Grelli[63], C. Grigoras[33],
V. Grigoriev[92], A. Grigoryan[1], S. Grigoryan[75], O.S. Groettvik[21], F. Grosa[30],
J.F. Grosse-Oetringhaus[33], R. Grosso[106], R. Guernane[78], M. Guittiere[114], K. Gulbrandsen[88],
T. Gunji[132], A. Gupta[100], R. Gupta[100], I.B. Guzman[44], R. Haake[146], M.K. Habib[106],
C. Hadjidakis[61], H. Hamagaki[81], G. Hamar[145], M. Hamid[6], R. Hannigan[119], M.R. Haque[63,85],
A. Harlenderova[106], J.W. Harris[146], A. Harton[11], J.A. Hasenbichler[33], H. Hassan[95],
D. Hatzifotiadou[10,53], P. Hauer[42], S. Hayashi[132], S.T. Heckel[68,104], E. Hellbär[68], H. Helstrup[35],
A. Herghelegiu[47], T. Herman[36], E.G. Hernandez[44], G. Herrera Corral[9], F. Herrmann[144],
K.F. Hetland[35], H. Hillemanns[33], C. Hills[127], B. Hippolyte[136], B. Hohlweger[104], J. Honermann[144],
D. Horak[36], A. Hornung[68], S. Hornung[106], R. Hosokawa[15], P. Hristov[33], C. Huang[61],
C. Hughes[130], P. Huhn[68], T.J. Humanic[96], H. Hushnud[109], L.A. Husova[144], N. Hussain[41],
S.A. Hussain[14], D. Hutter[38], J.P. Iddon[33,127], R. Ilkaev[108], M. Inaba[133], G.M. Innocenti[33],
M. Ippolitov[87], A. Isakov[94], M.S. Islam[109], M. Ivanov[106], V. Ivanov[97], V. Izucheev[90], B. Jacak[79],
N. Jacazio[53], P.M. Jacobs[79], S. Jadlovska[116], J. Jadlovsky[116], S. Jaelani[63], C. Jahnke[121],
M.J. Jakubowska[142], M.A. Janik[142], T. Janson[74], M. Jercic[98], O. Jevons[110], M. Jin[125],
F. Jonas[95,144], P.G. Jones[110], J. Jung[68], M. Jung[68], A. Jusko[110], P. Kalinak[64], A. Kalweit[33],
V. Kaplin[92], S. Kar[6], A. Karasu Uysal[77], O. Karavichev[62], T. Karavicheva[62], P. Karczmarczyk[33],
E. Karpechev[62], U. Kebschull[74], R. Keidel[46], M. Keil[33], B. Ketzer[42], Z. Khabanova[89],
A.M. Khan[6], S. Khan[16], S.A. Khan[141], A. Khanzadeev[97], Y. Kharlov[90], A. Khatun[16],
A. Khuntia[118], B. Kileng[35], B. Kim[60], B. Kim[133], D. Kim[147], D.J. Kim[126], E.J. Kim[73],
H. Kim[17,147], J. Kim[147], J.S. Kim[40], J. Kim[103], J. Kim[147], J. Kim[73], M. Kim[103], S. Kim[18],
T. Kim[147], T. Kim[147], S. Kirsch[38,68], I. Kisel[38], S. Kiselev[91], A. Kisiel[142], J.L. Klay[5], C. Klein[68],
J. Klein[58], S. Klein[79], C. Klein-Bösing[144], M. Kleiner[68], A. Kluge[33], M.L. Knichel[33],
A.G. Knospe[125], C. Kobdaj[115], M.K. Köhler[103], T. Kollegger[106], A. Kondratyev[75],
N. Kondratyeva[92], E. Kondratyuk[90], J. Konig[68], P.J. Konopka[33], L. Koska[116], O. Kovalenko[84],
V. Kovalenko[112], M. Kowalski[118], I. Králik[64], A. Kravčáková[37], L. Kreis[106], M. Krivda[64,110],
F. Krizek[94], K. Krizkova Gajdosova[36], M. Krüger[68], E. Kryshen[97], M. Krzewicki[38],
A.M. Kubera[96], V. Kučera[60], C. Kuhn[136], P.G. Kuijer[89], L. Kumar[99], S. Kundu[85],
P. Kurashvili[84], A. Kurepin[62], A.B. Kurepin[62], A. Kuryakin[108], S. Kushpil[94], J. Kvapil[110],
M.J. Kweon[60], J.Y. Kwon[60], Y. Kwon[147], S.L. La Pointe[38], P. La Rocca[27], Y.S. Lai[79],
R. Langoy[129], K. Lapidus[33], A. Lardeux[20], P. Larionov[51], E. Laudi[33], R. Lavicka[36],
T. Lazareva[112], R. Lea[24], L. Leardini[103], J. Lee[133], S. Lee[147], F. Lehas[89], S. Lehner[113],
J. Lehrbach[38], R.C. Lemmon[93], I. León Monzón[120], E.D. Lesser[19], M. Lettrich[33], P. Lévai[145],
X. Li[12], X.L. Li[6], J. Lien[129], R. Lietava[110], B. Lim[17], V. Lindenstruth[38], S.W. Lindsay[127],
C. Lippmann[106], M.A. Lisa[96], A. Liu[19], J. Liu[127], S. Liu[96], W.J. Llope[143], I.M. Lofnes[21],
V. Loginov[92], C. Loizides[95], P. Loncar[34], J.A.L. Lopez[103], X. Lopez[134], E. López Torres[8],
J.R. Luhder[144], M. Lunardon[28], G. Luparello[59], Y.G. Ma[39], A. Maevskaya[62], M. Mager[33],
S.M. Mahmood[20], T. Mahmoud[42], A. Maire[136], R.D. Majka[146], M. Malaev[97], Q.W. Malik[20],
L. Malinina[75, iv], D. Mal'Kevich[91], P. Malzacher[106], G. Mandaglio[55], V. Manko[87], F. Manso[134],
V. Manzari[52], Y. Mao[6], M. Marchisone[135], J. Mareš[66], G.V. Margagliotti[24], A. Margotti[53],
J. Margutti[63], A. Marín[106], C. Markert[119], M. Marquard[68], N.A. Martin[103], P. Martinengo[33],
J.L. Martinez[125], M.I. Martínez[44], G. Martínez García[114], M. Martinez Pedreira[33],

S. Masciocchi[106], M. Masera[25], A. Masoni[54], L. Massacrier[61], E. Masson[114], A. Mastroserio[52,138], A.M. Mathis[104,117], O. Matonoha[80], P.F.T. Matuoka[121], A. Matyja[118], C. Mayer[118], F. Mazzaschi[25], M. Mazzilli[52], M.A. Mazzoni[57], A.F. Mechler[68], F. Meddi[22], Y. Melikyan[62,92], A. Menchaca-Rocha[71], C. Mengke[6], E. Meninno[29,113], M. Meres[13], S. Mhlanga[124], Y. Miake[133], L. Micheletti[25], D.L. Mihaylov[104], K. Mikhaylov[75,91], A.N. Mishra[69], D. Miśkowiec[106], A. Modak[3], N. Mohammadi[33], A.P. Mohanty[63], B. Mohanty[85], M. Mohisin Khan[16, v], C. Mordasini[104], D.A. Moreira De Godoy[144], L.A.P. Moreno[44], I. Morozov[62], A. Morsch[33], T. Mrnjavac[33], V. Muccifora[51], E. Mudnic[34], D. Mühlheim[144], S. Muhuri[141], J.D. Mulligan[79], M.G. Munhoz[121], R.H. Munzer[68], H. Murakami[132], S. Murray[124], L. Musa[33], J. Musinsky[64], C.J. Myers[125], J.W. Myrcha[142], B. Naik[48], R. Nair[84], B.K. Nandi[48], R. Nania[10,53], E. Nappi[52], M.U. Naru[14], A.F. Nassirpour[80], C. Nattrass[130], R. Nayak[48], T.K. Nayak[85], S. Nazarenko[108], A. Neagu[20], R.A. Negrao De Oliveira[68], L. Nellen[69], S.V. Nesbo[35], G. Neskovic[38], D. Nesterov[112], L.T. Neumann[142], B.S. Nielsen[88], S. Nikolaev[87], S. Nikulin[87], V. Nikulin[97], F. Noferini[10,53], P. Nomokonov[75], J. Norman[78,127], N. Novitzky[133], P. Nowakowski[142], A. Nyanin[87], J. Nystrand[21], M. Ogino[81], A. Ohlson[80,103], J. Oleniacz[142], A.C. Oliveira Da Silva[121,130], M.H. Oliver[146], C. Oppedisano[58], R. Orava[43], A. Ortiz Velasquez[69], A. Oskarsson[80], J. Otwinowski[118], K. Oyama[81], Y. Pachmayer[103], V. Pacik[88], D. Pagano[140], G. Paić[69], J. Pan[143], A.K. Pandey[48], S. Panebianco[137], P. Pareek[49,141], J. Park[60], J.E. Parkkila[126], S. Parmar[99], S.P. Pathak[125], R.N. Patra[141], B. Paul[23], H. Pei[6], T. Peitzmann[63], X. Peng[6], L.G. Pereira[70], H. Pereira Da Costa[137], D. Peresunko[87], G.M. Perez[8], E. Perez Lezama[68], V. Peskov[68], Y. Pestov[4], V. Petráček[36], M. Petrovici[47], R.P. Pezzi[70], S. Piano[59], M. Pikna[13], P. Pillot[114], O. Pinazza[33,53], L. Pinsky[125], C. Pinto[27], S. Pisano[10,51], D. Pistone[55], M. Płoskoń[79], M. Planinic[98], F. Pliquett[68], S. Pochybova[145, i], M.G. Poghosyan[95], B. Polichtchouk[90], N. Poljak[98], A. Pop[47], H. Poppenborg[144], S. Porteboeuf-Houssais[134], V. Pozdniakov[75], S.K. Prasad[3], R. Preghenella[53], F. Prino[58], C.A. Pruneau[143], I. Pshenichnov[62], M. Puccio[25,33], J. Putschke[143], L. Quaglia[25], R.E. Quishpe[125], S. Ragoni[110], S. Raha[3], S. Rajput[100], J. Rak[126], A. Rakotozafindrabe[137], L. Ramello[31], F. Rami[136], R. Raniwala[101], S. Raniwala[101], S.S. Räsänen[43], R. Rath[49], V. Ratza[42], I. Ravasenga[89], K.F. Read[95,130], A.R. Redelbach[38], K. Redlich[84, vi], A. Rehman[21], P. Reichelt[68], F. Reidt[33], X. Ren[6], R. Renfordt[68], Z. Rescakova[37], J.-P. Revol[10], K. Reygers[103], V. Riabov[97], T. Richert[80,88], M. Richter[20], P. Riedler[33], W. Riegler[33], F. Riggi[27], C. Ristea[67], S.P. Rode[49], M. Rodríguez Cahuantzi[44], K. Røed[20], R. Rogalev[90], E. Rogochaya[75], D. Rohr[33], D. Röhrich[21], P.S. Rokita[142], F. Ronchetti[51], E.D. Rosas[69], K. Roslon[142], A. Rossi[28,56], A. Rotondi[139], A. Roy[49], P. Roy[109], O.V. Rueda[80], R. Rui[24], B. Rumyantsev[75], A. Rustamov[86], E. Ryabinkin[87], Y. Ryabov[97], A. Rybicki[118], H. Rytkonen[126], O.A.M. Saarimaki[43], S. Sadhu[141], S. Sadovsky[90], K. Šafařík[36], S.K. Saha[141], B. Sahoo[48], P. Sahoo[48], R. Sahoo[49], S. Sahoo[65], P.K. Sahu[65], J. Saini[141], S. Sakai[133], S. Sambyal[100], V. Samsonov[92,97], D. Sarkar[143], N. Sarkar[141], P. Sarma[41], V.M. Sarti[104], M.H.P. Sas[63], E. Scapparone[53], B. Schaefer[95], J. Schambach[119], H.S. Scheid[68], C. Schiaua[47], R. Schicker[103], A. Schmah[103], C. Schmidt[106], H.R. Schmidt[102], M.O. Schmidt[103], M. Schmidt[102], N.V. Schmidt[68,95], A.R. Schmier[130], J. Schukraft[88], Y. Schutz[33,136], K. Schwarz[106], K. Schweda[106], G. Scioli[26], E. Scomparin[58], M. Šefčík[37], J.E. Seger[15], Y. Sekiguchi[132], D. Sekihata[132], I. Selyuzhenkov[92,106], S. Senyukov[136], D. Serebryakov[62], E. Serradilla[71], A. Sevcenco[67], A. Shabanov[62], A. Shabetai[114], R. Shahoyan[33], W. Shaikh[109], A. Shangaraev[90], A. Sharma[99], A. Sharma[100], H. Sharma[118], M. Sharma[100], N. Sharma[99], S. Sharma[100], A.I. Sheikh[141], K. Shigaki[45], M. Shimomura[82], S. Shirinkin[91], Q. Shou[39], Y. Sibiriak[87], S. Siddhanta[54], T. Siemiarczuk[84], D. Silvermyr[80], G. Simatovic[89], G. Simonetti[33,104], R. Singh[85], R. Singh[100], R. Singh[49], V.K. Singh[141], V. Singhal[141], T. Sinha[109], B. Sitar[13], M. Sitta[31], T.B. Skaali[20], M. Slupecki[126], N. Smirnov[146], R.J.M. Snellings[63], T.W. Snellman[43,126], C. Soncco[111], J. Song[60,125], A. Songmoolnak[115], F. Soramel[28],

S. Sorensen[130], I. Sputowska[118], J. Stachel[103], I. Stan[67], P. Stankus[95], P.J. Steffanic[130],
E. Stenlund[80], D. Stocco[114], M.M. Storetvedt[35], L.D. Stritto[29], A.A.P. Suaide[121], T. Sugitate[45],
C. Suire[61], M. Suleymanov[14], M. Suljic[33], R. Sultanov[91], M. Šumbera[94], V. Sumberia[100],
S. Sumowidagdo[50], S. Swain[65], A. Szabo[13], I. Szarka[13], U. Tabassam[14], S.F. Taghavi[104],
G. Taillepied[134], J. Takahashi[122], G.J. Tambave[21], S. Tang[6,134], M. Tarhini[114], M.G. Tarzila[47],
A. Tauro[33], G. Tejeda Muñoz[44], A. Telesca[33], L. Terlizzi[25], C. Terrevoli[125], D. Thakur[49],
S. Thakur[141], D. Thomas[119], F. Thoresen[88], R. Tieulent[135], A. Tikhonov[62], A.R. Timmins[125],
A. Toia[68], N. Topilskaya[62], M. Toppi[51], F. Torales-Acosta[19], S.R. Torres[36,120], A. Trifiro[55],
S. Tripathy[49], T. Tripathy[48], S. Trogolo[28], G. Trombetta[32], L. Tropp[37], V. Trubnikov[2],
W.H. Trzaska[126], T.P. Trzcinski[142], B.A. Trzeciak[36,63], T. Tsuji[132], A. Tumkin[108], R. Turrisi[56],
T.S. Tveter[20], K. Ullaland[21], E.N. Umaka[125], A. Uras[135], G.L. Usai[23], A. Utrobicic[98], M. Vala[37],
N. Valle[139], S. Vallero[58], N. van der Kolk[63], L.V.R. van Doremalen[63], M. van Leeuwen[63],
P. Vande Vyvre[33], D. Varga[145], Z. Varga[145], M. Varga-Kofarago[145], A. Vargas[44], M. Vasileiou[83],
A. Vasiliev[87], O. Vázquez Doce[104,117], V. Vechernin[112], A.M. Veen[63], E. Vercellin[25], S. Vergara
Limón[44], L. Vermunt[63], R. Vernet[7], R. Vértesi[145], L. Vickovic[34], Z. Vilakazi[131], O. Villalobos
Baillie[110], A. Villatoro Tello[44], G. Vino[52], A. Vinogradov[87], T. Virgili[29], V. Vislavicius[88],
A. Vodopyanov[75], B. Volkel[33], M.A. Völkl[102], K. Voloshin[91], S.A. Voloshin[143], G. Volpe[32], B. von
Haller[33], I. Vorobyev[104], D. Voscek[116], J. Vrláková[37], B. Wagner[21], M. Weber[113], A. Wegrzynek[33],
D.F. Weiser[103], S.C. Wenzel[33], J.P. Wessels[144], J. Wiechula[68], J. Wikne[20], G. Wilk[84],
J. Wilkinson[10,53], G.A. Willems[144], E. Willsher[110], B. Windelband[103], M. Winn[137], W.E. Witt[130],
Y. Wu[128], R. Xu[6], S. Yalcin[77], Y. Yamaguchi[45], K. Yamakawa[45], S. Yang[21], S. Yano[137], Z. Yin[6],
H. Yokoyama[63], I.-K. Yoo[17], J.H. Yoon[60], S. Yuan[21], A. Yuncu[103], V. Yurchenko[2], V. Zaccolo[24],
A. Zaman[14], C. Zampolli[33], H.J.C. Zanoli[63], N. Zardoshti[33], A. Zarochentsev[112], P. Závada[66],
N. Zaviyalov[108], H. Zbroszczyk[142], M. Zhalov[97], S. Zhang[39], X. Zhang[6], Z. Zhang[6],
V. Zherebchevskii[112], D. Zhou[6], Y. Zhou[88], Z. Zhou[21], J. Zhu[6,106], Y. Zhu[6], A. Zichichi[10,26],
M.B. Zimmermann[33], G. Zinovjev[2], N. Zurlo[140],

[i] *Deceased*
[ii] *Italian National Agency for New Technologies, Energy and Sustainable Economic Development (ENEA), Bologna, Italy*
[iii] *Dipartimento DET del Politecnico di Torino, Turin, Italy*
[iv] *M.V. Lomonosov Moscow State University, D.V. Skobeltsyn Institute of Nuclear, Physics, Moscow, Russia*
[v] *Department of Applied Physics, Aligarh Muslim University, Aligarh, India*
[vi] *Institute of Theoretical Physics, University of Wroclaw, Poland*

[1] *A.I. Alikhanyan National Science Laboratory (Yerevan Physics Institute) Foundation, Yerevan, Armenia*
[2] *Bogolyubov Institute for Theoretical Physics, National Academy of Sciences of Ukraine, Kiev, Ukraine*
[3] *Bose Institute, Department of Physics and Centre for Astroparticle Physics and Space Science (CAPSS), Kolkata, India*
[4] *Budker Institute for Nuclear Physics, Novosibirsk, Russia*
[5] *California Polytechnic State University, San Luis Obispo, California, United States*
[6] *Central China Normal University, Wuhan, China*
[7] *Centre de Calcul de l'IN2P3, Villeurbanne, Lyon, France*
[8] *Centro de Aplicaciones Tecnológicas y Desarrollo Nuclear (CEADEN), Havana, Cuba*
[9] *Centro de Investigación y de Estudios Avanzados (CINVESTAV), Mexico City and Mérida, Mexico*
[10] *Centro Fermi — Museo Storico della Fisica e Centro Studi e Ricerche "Enrico Fermi', Rome, Italy*

[11] *Chicago State University, Chicago, Illinois, United States*
[12] *China Institute of Atomic Energy, Beijing, China*
[13] *Comenius University Bratislava, Faculty of Mathematics, Physics and Informatics, Bratislava, Slovakia*
[14] *COMSATS University Islamabad, Islamabad, Pakistan*
[15] *Creighton University, Omaha, Nebraska, United States*
[16] *Department of Physics, Aligarh Muslim University, Aligarh, India*
[17] *Department of Physics, Pusan National University, Pusan, Republic of Korea*
[18] *Department of Physics, Sejong University, Seoul, Republic of Korea*
[19] *Department of Physics, University of California, Berkeley, California, United States*
[20] *Department of Physics, University of Oslo, Oslo, Norway*
[21] *Department of Physics and Technology, University of Bergen, Bergen, Norway*
[22] *Dipartimento di Fisica dell'Università 'La Sapienza' and Sezione INFN, Rome, Italy*
[23] *Dipartimento di Fisica dell'Università and Sezione INFN, Cagliari, Italy*
[24] *Dipartimento di Fisica dell'Università and Sezione INFN, Trieste, Italy*
[25] *Dipartimento di Fisica dell'Università and Sezione INFN, Turin, Italy*
[26] *Dipartimento di Fisica e Astronomia dell'Università and Sezione INFN, Bologna, Italy*
[27] *Dipartimento di Fisica e Astronomia dell'Università and Sezione INFN, Catania, Italy*
[28] *Dipartimento di Fisica e Astronomia dell'Università and Sezione INFN, Padova, Italy*
[29] *Dipartimento di Fisica 'E.R. Caianiello' dell'Università and Gruppo Collegato INFN, Salerno, Italy*
[30] *Dipartimento DISAT del Politecnico and Sezione INFN, Turin, Italy*
[31] *Dipartimento di Scienze e Innovazione Tecnologica dell'Università del Piemonte Orientale and INFN Sezione di Torino, Alessandria, Italy*
[32] *Dipartimento Interateneo di Fisica 'M. Merlin' and Sezione INFN, Bari, Italy*
[33] *European Organization for Nuclear Research (CERN), Geneva, Switzerland*
[34] *Faculty of Electrical Engineering, Mechanical Engineering and Naval Architecture, University of Split, Split, Croatia*
[35] *Faculty of Engineering and Science, Western Norway University of Applied Sciences, Bergen, Norway*
[36] *Faculty of Nuclear Sciences and Physical Engineering, Czech Technical University in Prague, Prague, Czech Republic*
[37] *Faculty of Science, P.J. Šafárik University, Košice, Slovakia*
[38] *Frankfurt Institute for Advanced Studies, Johann Wolfgang Goethe-Universität Frankfurt, Frankfurt, Germany*
[39] *Fudan University, Shanghai, China*
[40] *Gangneung-Wonju National University, Gangneung, Republic of Korea*
[41] *Gauhati University, Department of Physics, Guwahati, India*
[42] *Helmholtz-Institut für Strahlen- und Kernphysik, Rheinische Friedrich-Wilhelms-Universität Bonn, Bonn, Germany*
[43] *Helsinki Institute of Physics (HIP), Helsinki, Finland*
[44] *High Energy Physics Group, Universidad Autónoma de Puebla, Puebla, Mexico*
[45] *Hiroshima University, Hiroshima, Japan*
[46] *Hochschule Worms, Zentrum für Technologietransfer und Telekommunikation (ZTT), Worms, Germany*
[47] *Horia Hulubei National Institute of Physics and Nuclear Engineering, Bucharest, Romania*
[48] *Indian Institute of Technology Bombay (IIT), Mumbai, India*
[49] *Indian Institute of Technology Indore, Indore, India*
[50] *Indonesian Institute of Sciences, Jakarta, Indonesia*
[51] *INFN, Laboratori Nazionali di Frascati, Frascati, Italy*
[52] *INFN, Sezione di Bari, Bari, Italy*
[53] *INFN, Sezione di Bologna, Bologna, Italy*
[54] *INFN, Sezione di Cagliari, Cagliari, Italy*

⁵⁵ *INFN, Sezione di Catania, Catania, Italy*

⁵⁶ *INFN, Sezione di Padova, Padova, Italy*

⁵⁷ *INFN, Sezione di Roma, Rome, Italy*

⁵⁸ *INFN, Sezione di Torino, Turin, Italy*

⁵⁹ *INFN, Sezione di Trieste, Trieste, Italy*

⁶⁰ *Inha University, Incheon, Republic of Korea*

⁶¹ *Institut de Physique Nucléaire d'Orsay (IPNO), Institut National de Physique Nucléaire et de Physique des Particules (IN2P3/CNRS), Université de Paris-Sud, Université Paris-Saclay, Orsay, France*

⁶² *Institute for Nuclear Research, Academy of Sciences, Moscow, Russia*

⁶³ *Institute for Subatomic Physics, Utrecht University/Nikhef, Utrecht, Netherlands*

⁶⁴ *Institute of Experimental Physics, Slovak Academy of Sciences, Košice, Slovakia*

⁶⁵ *Institute of Physics, Homi Bhabha National Institute, Bhubaneswar, India*

⁶⁶ *Institute of Physics of the Czech Academy of Sciences, Prague, Czech Republic*

⁶⁷ *Institute of Space Science (ISS), Bucharest, Romania*

⁶⁸ *Institut für Kernphysik, Johann Wolfgang Goethe-Universität Frankfurt, Frankfurt, Germany*

⁶⁹ *Instituto de Ciencias Nucleares, Universidad Nacional Autónoma de México, Mexico City, Mexico*

⁷⁰ *Instituto de Física, Universidade Federal do Rio Grande do Sul (UFRGS), Porto Alegre, Brazil*

⁷¹ *Instituto de Física, Universidad Nacional Autónoma de México, Mexico City, Mexico*

⁷² *iThemba LABS, National Research Foundation, Somerset West, South Africa*

⁷³ *Jeonbuk National University, Jeonju, Republic of Korea*

⁷⁴ *Johann-Wolfgang-Goethe Universität Frankfurt Institut für Informatik, Fachbereich Informatik und Mathematik, Frankfurt, Germany*

⁷⁵ *Joint Institute for Nuclear Research (JINR), Dubna, Russia*

⁷⁶ *Korea Institute of Science and Technology Information, Daejeon, Republic of Korea*

⁷⁷ *KTO Karatay University, Konya, Turkey*

⁷⁸ *Laboratoire de Physique Subatomique et de Cosmologie, Université Grenoble-Alpes, CNRS-IN2P3, Grenoble, France*

⁷⁹ *Lawrence Berkeley National Laboratory, Berkeley, California, United States*

⁸⁰ *Lund University Department of Physics, Division of Particle Physics, Lund, Sweden*

⁸¹ *Nagasaki Institute of Applied Science, Nagasaki, Japan*

⁸² *Nara Women's University (NWU), Nara, Japan*

⁸³ *National and Kapodistrian University of Athens, School of Science, Department of Physics, Athens, Greece*

⁸⁴ *National Centre for Nuclear Research, Warsaw, Poland*

⁸⁵ *National Institute of Science Education and Research, Homi Bhabha National Institute, Jatni, India*

⁸⁶ *National Nuclear Research Center, Baku, Azerbaijan*

⁸⁷ *National Research Centre Kurchatov Institute, Moscow, Russia*

⁸⁸ *Niels Bohr Institute, University of Copenhagen, Copenhagen, Denmark*

⁸⁹ *Nikhef, National institute for subatomic physics, Amsterdam, Netherlands*

⁹⁰ *NRC Kurchatov Institute IHEP, Protvino, Russia*

⁹¹ *NRC "Kurchatov Institute" — ITEP, Moscow, Russia*

⁹² *NRNU Moscow Engineering Physics Institute, Moscow, Russia*

⁹³ *Nuclear Physics Group, STFC Daresbury Laboratory, Daresbury, United Kingdom*

⁹⁴ *Nuclear Physics Institute of the Czech Academy of Sciences, Řež u Prahy, Czech Republic*

⁹⁵ *Oak Ridge National Laboratory, Oak Ridge, Tennessee, United States*

⁹⁶ *Ohio State University, Columbus, Ohio, United States*

⁹⁷ *Petersburg Nuclear Physics Institute, Gatchina, Russia*

⁹⁸ *Physics department, Faculty of science, University of Zagreb, Zagreb, Croatia*

⁹⁹ *Physics Department, Panjab University, Chandigarh, India*

¹⁰⁰ *Physics Department, University of Jammu, Jammu, India*

¹⁰¹ *Physics Department, University of Rajasthan, Jaipur, India*

[102] *Physikalisches Institut, Eberhard-Karls-Universität Tübingen, Tübingen, Germany*
[103] *Physikalisches Institut, Ruprecht-Karls-Universität Heidelberg, Heidelberg, Germany*
[104] *Physik Department, Technische Universität München, Munich, Germany*
[105] *Politecnico di Bari, Bari, Italy*
[106] *Research Division and ExtreMe Matter Institute EMMI, GSI Helmholtzzentrum für Schwerionenforschung GmbH, Darmstadt, Germany*
[107] *Rudjer Bošković Institute, Zagreb, Croatia*
[108] *Russian Federal Nuclear Center (VNIIEF), Sarov, Russia*
[109] *Saha Institute of Nuclear Physics, Homi Bhabha National Institute, Kolkata, India*
[110] *School of Physics and Astronomy, University of Birmingham, Birmingham, United Kingdom*
[111] *Sección Física, Departamento de Ciencias, Pontificia Universidad Católica del Perú, Lima, Peru*
[112] *St. Petersburg State University, St. Petersburg, Russia*
[113] *Stefan Meyer Institut für Subatomare Physik (SMI), Vienna, Austria*
[114] *SUBATECH, IMT Atlantique, Université de Nantes, CNRS-IN2P3, Nantes, France*
[115] *Suranaree University of Technology, Nakhon Ratchasima, Thailand*
[116] *Technical University of Košice, Košice, Slovakia*
[117] *Technische Universität München, Excellence Cluster 'Universe', Munich, Germany*
[118] *The Henryk Niewodniczanski Institute of Nuclear Physics, Polish Academy of Sciences, Cracow, Poland*
[119] *The University of Texas at Austin, Austin, Texas, United States*
[120] *Universidad Autónoma de Sinaloa, Culiacán, Mexico*
[121] *Universidade de São Paulo (USP), São Paulo, Brazil*
[122] *Universidade Estadual de Campinas (UNICAMP), Campinas, Brazil*
[123] *Universidade Federal do ABC, Santo Andre, Brazil*
[124] *University of Cape Town, Cape Town, South Africa*
[125] *University of Houston, Houston, Texas, United States*
[126] *University of Jyväskylä, Jyväskylä, Finland*
[127] *University of Liverpool, Liverpool, United Kingdom*
[128] *University of Science and Technology of China, Hefei, China*
[129] *University of South-Eastern Norway, Tonsberg, Norway*
[130] *University of Tennessee, Knoxville, Tennessee, United States*
[131] *University of the Witwatersrand, Johannesburg, South Africa*
[132] *University of Tokyo, Tokyo, Japan*
[133] *University of Tsukuba, Tsukuba, Japan*
[134] *Université Clermont Auvergne, CNRS/IN2P3, LPC, Clermont-Ferrand, France*
[135] *Université de Lyon, Université Lyon 1, CNRS/IN2P3, IPN-Lyon, Villeurbanne, Lyon, France*
[136] *Université de Strasbourg, CNRS, IPHC UMR 7178, F-67000 Strasbourg, France, Strasbourg, France*
[137] *Université Paris-Saclay Centre d'Etudes de Saclay (CEA), IRFU, Départment de Physique Nucléaire (DPhN), Saclay, France*
[138] *Università degli Studi di Foggia, Foggia, Italy*
[139] *Università degli Studi di Pavia, Pavia, Italy*
[140] *Università di Brescia, Brescia, Italy*
[141] *Variable Energy Cyclotron Centre, Homi Bhabha National Institute, Kolkata, India*
[142] *Warsaw University of Technology, Warsaw, Poland*
[143] *Wayne State University, Detroit, Michigan, United States*
[144] *Westfälische Wilhelms-Universität Münster, Institut für Kernphysik, Münster, Germany*
[145] *Wigner Research Centre for Physics, Budapest, Hungary*
[146] *Yale University, New Haven, Connecticut, United States*
[147] *Yonsei University, Seoul, Republic of Korea*